When is natural convection completely passive?

When is natural convection completely passive?

ANTHONY KAY

Department of Mathematical Sciences, Loughborough University,

Loughborough, Leicestershire, LE11 3TU

Tel: +44 1509 222878

Fax: +44 1509 223969

Email: A.Kay@Lboro.ac.uk

Abstract

Momentum and energy equations for vertical flow, including viscous dissipation and pressure work, are derived and shown to require that the cross-section mean density is taken as the reference density for calculation of buoyancy forces under the Boussinesq approximation. Solutions are obtained for flow between parallel plane walls, with and without the pressure work as an explicit term in the energy equation. Both walls are at the same temperature, so there is no thermal forcing, but solutions are obtained for all admissible values of dynamic pressure gradient. The passive convection condition, whereby the flow is driven entirely by buoyancy forces resulting from heat generated by the flow's own viscous dissipation, is found on one branch of the dual solutions. However, while theoretically possible, passive convection is not physically realisable with any real fluid.

1 Introduction

Viscous dissipation raises the temperature of a fluid; spatial variations in temperature result in buoyancy forces, which can then drive a flow. Thus we may conceive of a flow which is sustained by the buoyancy forces resulting from the flow's own viscous dissipation, without any external heating or applied pressure gradient. Such a flow was denoted "Completely passive natural convection" by Miklavčič and Wang [1] (hereafter MW); we shall use the briefer designation, "passive convection". MW obtained solutions of equations which they claimed to represent steady passive convection flows in vertical ducts with walls held at a uniform temperature.

Schneider [2] subsequently responded with several objections, which may be summarised as follows:-

1. The flow appears to violate the First Law of Thermodynamics (as well as the Second Law). The temperature profile calculated by MW, with a negative temperature gradient at the duct wall, implies conduction of heat out through the wall; yet there is no input of either heat or work.

2. The hydrostatic pressure gradient within the duct will not balance the ambient hydrostatic pressure gradient because the mean temperature within the duct is not equal to the ambient temperature. Thus MW's choice of the duct wall temperature (assumed equal to the ambient temperature) as their reference temperature entails an input of either heat or work, the former to warm the fluid from the ambient to the internal mean temperature, or the latter by means of an applied pressure gradient to equalise the internal and ambient pressures; so the convection is not passive.

3. The pressure work term in the energy equation, which gives the work done on a compressible fluid as it moves down a pressure gradient, has been neglected when it may be as significant as the viscous dissipation term.

4. The orders of magnitude of fluid properties (specific heats, viscosity, etc.) for any real fluid would make the flow extremely difficult to realise in practice.

The second objection has fundamental implications for the modeling of free and forced convection flows in vertical ducts. A variety of choices of reference temperature may be found in the literature, even in work published after Barletta and Zanchini [3] pointed out the necessity for choosing the cross-section mean temperature. This provides the main motivation for the present work: in Section 2 we provide a re-derivation of the momentum equation for convection flows in vertical ducts, to provide a rational basis for this choice of reference temperature. In Section 3 we discuss the energy equation, including the pressure work term (the subject of Schneider's third objection) and also allowing for thermodynamically closed systems (insulated walls or specified heat flux at the walls) as well as open systems where the boundary heat flux is determined in response to other specified conditions. Our recommendations for the formulation of the momentum equation have implications for the specification of boundary conditions and for procedures to solve the resulting boundary value problems; these are discussed in Section 4. After making the equations dimensionless in Section 5, solutions are presented for the case of two-dimensional flow between parallel vertical walls with symmetric and thermodynamically open conditions in Section 6. Some of the velocity and

temperature profiles presented here have appeared previously in the literature: a solution with a differently specified reference temperature may yield similar profiles, but associated with a different value of applied pressure gradient. Nevertheless, there is considerable novel mathematical development in Section 6, as well as a more thorough analysis of how the flow responds to the complete range of applied pressure gradients (including the "passive convection" case) than has appeared previously, and our calculations including pressure work appear to be entirely new.

Schneider [2] attributed the thermodynamic paradox (his first objection above) to the error in the choice of reference temperature. However, we shall show that when our recommendation for this choice is followed, a passive convection solution is still available; the temperature profile still yields what Schneider describes as "a particularly nice version of a perpetuum mobile", allowing us to extract heat from the system when there is no energy input. Furthermore, including the pressure work term still allows such a flow; Miklavčič and Wang [4] re-calculated their flow with this term included, finding that it made only a minor adjustment to their original results, and our more thorough calculations with our choice of reference temperature confirm that a passive convection solution still exists when pressure work is accounted for. In fact, Schneider's observation that heat "has to be removed from the duct by cooling the walls" is sufficient to resolve the paradox. We discuss this in more detail in Section 7, where we also comment on the problem of realising passive convection with real fluids (Schneider's fourth objection).

2 Momentum equation

MW wrote down an equation expressing a balance between viscous and buoyancy forces for steady, unidirectional flow with vertical velocity W and temperature T:

$$\mu \frac{\mathrm{d}^2 W}{\mathrm{d}Y^2} + \rho_0 g \beta (T - T_a) = 0, \tag{1}$$

where the viscosity μ, density ρ_0 and coefficient of thermal expansion β are all assumed constant under the Boussinesq approximation. This form applies for flow between parallel

plane walls at $Y = \pm L$, with no variation in the spanwise (X) direction; MW also wrote down the corresponding equation for axisymmetric flow in a duct of circular cross-section. The flow described by (1) is claimed to be completely passive on the basis that all walls are at a uniform temperature equal to the reference temperature T_a in (1), and no pressure gradient appears in the equation.

Let us now consider the derivation of (1), but in the more general form applicable to a vertical duct of uniform but arbitrary cross-section S with perimeter C; we use the respective symbols S and C to denote the area of the cross-section and the length of the perimeter as well as to indicate the domain of integration in the symbols $\int_S$ and $\oint_C$. The notations ∇_h and ∇_h^2 will be used for the horizontal gradient operator and the horizontal Laplacian respectively, i.e. (in Cartesian coordinates)

$$\nabla_h = \left(\frac{\partial}{\partial X}, \frac{\partial}{\partial Y}\right), \qquad \nabla_h^2 = \frac{\partial^2}{\partial X^2} + \frac{\partial^2}{\partial Y^2}\,. \tag{2}$$

To apply the theory below to the two-dimensional case where the duct has parallel plane walls at $Y = -L$ and $Y = L$, it is only necessary to change the notations:-

$$\int_S \cdot\, \mathrm{d}S \to \int_{-L}^{L} \cdot\, \mathrm{d}Y\,, \qquad \oint_C \cdot\, \mathrm{d}l \to [\cdot]_{-L}^{L}\,, \qquad \nabla_h \to \frac{\mathrm{d}}{\mathrm{d}Y}\,, \qquad \nabla_h^2 \to \frac{\mathrm{d}}{\mathrm{d}Y^2}\,.$$

We assume solenoidal, unidirectional flow in the vertical (Z) direction, so that

$$\frac{\partial W}{\partial Z} = 0 \tag{3}$$

and the Navier-Stokes equations reduce to

$$\nabla_h P = 0\,, \tag{4}$$

$$-\frac{\mathrm{d}P}{\mathrm{d}Z} - \rho g + \mu \nabla_h^2 W = 0\,. \tag{5}$$

If the density ρ was horizontally uniform, we could have hydrostatic equilibrium, $W \equiv 0$ with $\mathrm{d}P/\mathrm{d}Z = -\rho g$. When ρ is non-uniform, there are buoyancy forces, and $W \neq 0$. In any flow involving body forces, we separate the pressure gradient into a hydrostatic part, which

supports the weight of the fluid (in the case where the body force is gravity), and a dynamic part, which is involved in the motion of the fluid:

$$P = P_h + P_d \,. \tag{6}$$

With zero horizontal flow component, the horizontal component of the dynamic pressure gradient must obviously be zero; this is also true of the total pressure gradient (see (4)), and hence the hydrostatic pressure is horizontally uniform. With the density varying horizontally, the only sense in which the hydrostatic pressure gradient can then be said to support the weight of the fluid is if we consider the entire cross-section S of the duct:

$$\int_S \frac{\mathrm{d}P_h}{\mathrm{d}Z}\,\mathrm{d}S = -g\int_S \rho\,\mathrm{d}S\,, \tag{7}$$

so that

$$\frac{\mathrm{d}P_h}{\mathrm{d}Z} = -\rho_m g \tag{8}$$

where ρ_m is the mean density over the cross-section. Applying (6) and (8) to (5), we obtain the equation of motion in the form

$$-\frac{\mathrm{d}P_d}{\mathrm{d}Z} - (\rho - \rho_m)g + \mu\nabla_h^2 W = 0\,. \tag{9}$$

Thus ρ_m has become the reference density for the calculation of the buoyancy force.

If we now integrate (9) over the cross-section, using the divergence theorem on the viscous term and noting that $\mathrm{d}P_d/\mathrm{d}Z$ is uniform over S, we obtain

$$S\frac{\mathrm{d}P_d}{\mathrm{d}Z} = \mu\oint_C \frac{\partial W}{\partial n}\,\mathrm{d}l\,, \tag{10}$$

where $\partial/\partial n$ denotes the derivative in the direction normal to the wall C. This equation says that the dynamic pressure gradient balances the viscous shear stress at the duct wall, a result which is well known for simple Poiseuille flow and is intuitively reasonable. Note that this does not apply if any density other than the cross-section mean ρ_m is chosen as the reference density. If the density is a linear function of temperature,

$$\rho = \rho_m(1 - \beta(T - T_m))\,, \tag{11}$$

we recover the result of Barletta & Zanchini [3], that the cross-sectional mean temperature should be used as the reference temperature for calculation of buoyancy forces. While these authors do not use the simple intuitive argument given above, they do demonstrate that any other choice of reference temperature is liable to imply that the dynamic pressure gradient takes a physically unreasonable form. Note also that our requirement on the reference density is more general than Barletta & Zanchini's requirement on temperature, since ours allows for a nonlinear relation between temperature and density, as found for example in cold water [5].

Equation (1), in which the wall temperature is used as the reference temperature, does not satisfy our requirement. In fact it disguises the presence of a dynamic pressure gradient of magnitude $\rho_0 g\beta(T_m - T_a)$, and so does not represent completely passive natural convection as claimed by MW. Equivalently we could say, following Schneider [2], that to obtain a balanced hydrostatic pressure some energy input is required to warm the incoming fluid from temperature T_a to the "mixing temperature", T_m. A momentum equation satisfying our requirement is obtained (for a duct of general cross-section) by inserting an equation of state into (9): for the linear case (11) this yields

$$-\frac{\mathrm{d}P_d}{\mathrm{d}Z} + \rho_m g\beta(T - T_m) + \mu\nabla_h^2 W = 0\,. \tag{12}$$

The convection can only be described as passive if $\mathrm{d}P_d/\mathrm{d}Z = 0$ in this equation.

We may ask, what justification might there be for using the wall temperature as a reference temperature? In one of the earliest contributions on convection in vertical ducts, Ostrach [6] referred specifically to a duct of large but finite length, open at the top and bottom to an ambient in hydrostatic equilibrium. In this case, the obvious choice of reference density is the density of the ambient. In a long duct, it is expected that there will be a substantial region of fully developed flow (unidirectional and not varying along the duct), but more complicated flows in the entry and exit regions. Ostrach's calculation is valid for the fully developed region, and ignores any energy input related to the flow in the entry and exit regions. If MW's "completely passive convection" flow was set up within the fully developed region, but with entry and exit regions at a temperature T_a different from

the cross-section mean, the flow would be gradually extinguished in the absence of some external energy input. Hence a passive convection flow could only exist in an infinitely long duct, or with entry and exit regions having exactly the same flow and temperature profiles as within the duct [2].

This also has implications for the Boussinesq approximation, which has already been used in two ways: firstly, in allowing density to vary with temperature while assuming solenoidal flow, and secondly in assuming that the viscosity μ and expansion coefficient β are constants. The thermal conductivity and specific heats will also be assumed constant when we derive the energy equation (Section 3 below), and these various fluid properties, together with the cross-section mean temperature T_m and density ρ_m, are also assumed constant where they are used in constructing reference quantities for nondimensionalisation in Section 5. All the fluid properties are in fact temperature-dependent, but if cross-sectional variations of temperature are small compared to absolute temperatures, the approximation by constant values may be sound. However, depending on the boundary conditions, it is possible to have a fully developed flow with the cross-section mean temperature T_m and density ρ_m varying linearly in the streamwise direction along the duct [7], provided that the buoyancy force, proportional to $T - T_m$ in (12), remains streamwise invariant. [We show below that passive convection is impossible in circumstances where T_m and ρ_m vary streamwise, but the implications for the Boussinesq approximation are worth discussing for more general cases.] The Boussinesq approximation is obviously incompatible with linearly varying T_m in an infinite duct, so we would have to imagine a finite duct with entry and exit conditions that do not disturb the fully developed flow.

3 Energy equation

MW's energy equation expressed a balance between the generation of heat by viscous dissipation and its transfer by horizontal conduction. For a duct of arbitrary cross-section, this

balance may be written

$$k\nabla_h^2 T + \mu(\nabla_h W).(\nabla_h W) = 0, \tag{13}$$

where k is the conductivity of heat (not the diffusivity as stated by MW). However, in general the two terms may not be in balance, so the entropy of fluid elements will change. This may be expressed in the equations,

$$c_p\rho\frac{\mathrm{d}T}{\mathrm{d}t} - \beta T\,\frac{\mathrm{d}P}{\mathrm{d}t} = T\frac{\mathrm{d}S}{\mathrm{d}t} = k\nabla_h^2 T + \mu(\nabla_h W).(\nabla_h W) \tag{14}$$

(see, for example, Batchelor's [8] equation (3.4.11)), where we have retained the form appropriate to unidirectional flow along a duct on the right, although the terms on the left are written in a more general form. The second term on the left is generally known as "pressure work"; in meteorology, the balance between this and the temperature change term accounts for the cooling of an air parcel rising isentropically and expanding as its pressure decreases. However, in the context of thermal convection calculations using the Boussinesq approximation, Barletta [9, 10] has recently discussed the energy balance in flows involving viscous dissipation and has concluded that the most appropriate form of energy equation excludes the pressure work term but may require a different specific heat to replace c_p in the temperature change term, depending on the properties of the fluid being considered. However, other authors [2, 11] insist on the importance of retaining the pressure work term. Rather than entering this discussion, we shall do calculations firstly with this term neglected, and then with it retained, so that we can evaluate its importance in the flow under consideration. The issue of which specific heat to use is of less importance since our detailed calculations will only require that the specific heat is constant.

Further insight into the energy balance can be gained by integrating (14) over the duct cross-section. Using the divergence theorem and Fourier's Law,

$$\int_S k\nabla_h^2 T\,\mathrm{d}S = -\oint_C Q\,\mathrm{d}l \tag{15}$$

where Q is the heat flux per unit horizontal distance along the duct perimeter. One of Green's identities, together with the no-slip condition, yields

$$\int_S (\nabla_h W).(\nabla_h W)\,\mathrm{d}S = -\int_S W\nabla_h^2 W\,\mathrm{d}S\,. \tag{16}$$

If the Boussinesq approximation is valid and the flow is vertical, the dominant contribution to the pressure work term in (14) will be from the hydrostatic pressure gradient, so

$$-\beta T \frac{\mathrm{d}P}{\mathrm{d}t} \approx -\beta T W \frac{\mathrm{d}P_h}{\mathrm{d}Z} \approx \beta T_m W \rho_m g \tag{17}$$

(with the approximation $T =$ constant suggested by Schneider [2], although he used T_a rather than T_m). Hence the integrated form of (14) is

$$\int_S c_p \rho \frac{\mathrm{d}T}{\mathrm{d}t} \,\mathrm{d}S = \int_S \beta T W \frac{\mathrm{d}P_h}{\mathrm{d}Z} - \oint_C Q \,\mathrm{d}l - \mu \int_S W \nabla_h^2 W \,\mathrm{d}S \,. \tag{18}$$

Substituting from the dynamical equation (12) in the last term of (18), we obtain

$$\int_S c_p \rho \frac{\mathrm{d}T}{\mathrm{d}t} \,\mathrm{d}S = -\oint_C Q \,\mathrm{d}l + \int_S W \left(\beta T \frac{\mathrm{d}P_h}{\mathrm{d}Z} - \frac{\mathrm{d}P_d}{\mathrm{d}Z} + \rho_m g \beta (T - T_m) \right) \mathrm{d}S \;: \tag{19}$$

the last integral includes the work done by the dynamic pressure gradient and buoyancy force in moving the fluid as well as the pressure work due to fluid rising through the hydrostatic pressure gradient. According to (19), if this work is not in balance with heat conduction through the duct walls, the imbalance will result in an increase or decrease of the fluid temperature. This is more generally applicable than the balance between viscous dissipation within the duct and heat transfer across its walls obtained by Barletta, Lazzari and Magyari [12]. If the boundary conditions do not specify Q on all boundaries, the heat flux can adjust to balance the work, and no temperature change is necessary; but if the heat flux is prescribed on all walls, the temperature of the fluid will in general need to change. It is usually assumed that this will be solely by fluid becoming warmer (or cooler) as it moves downstream, i.e.

$$\frac{\mathrm{d}T}{\mathrm{d}t} = W \frac{\partial T}{\partial Z} \,, \tag{20}$$

but it is also possible for there to be a local increase in temperature:

$$\frac{\mathrm{d}T}{\mathrm{d}t} = \frac{\partial T}{\partial t} + W \frac{\partial T}{\partial Z} \,. \tag{21}$$

Buoyancy forces depend on spatial variations of temperature, so steady, fully developed flow is possible if both $\partial T/\partial t$ and $\partial T/\partial Z$ are uniform throughout the fluid. Hence we may substitute

$$c_p \rho \frac{\mathrm{d}T}{\mathrm{d}t} = H + WG \tag{22}$$

in (14), where H and G are both constant and defined by

$$H = c\rho_m \frac{\partial T}{\partial t} \quad \text{and} \quad G = c\rho_m \frac{\partial T}{\partial Z}\,. \tag{23}$$

Here we have applied the Boussinesq approximation to replace ρ in (14) with the reference density ρ_m, and we have allowed for Barletta's [10] formulation by replacing c_p with an unspecified but constant specific heat c. Note that the term WG in (22) has the same mathematical form ($W \times$constant) as the pressure work term in (17). However, the constants in (17) are fixed and the term is present regardless of the boundary conditions, whereas G may only be required to be non-zero when heat fluxes are prescribed on all boundaries, and it is then diagnosed from the solution for the flow in the duct. [Note also that a non-zero streamwise temperature gradient (i.e. non-zero G) in a long duct may be inconsistent both with the approximation $T \approx T_m$ used in (17) and with the Boussinesq approximation.]

We may write the integral energy equation (19) in terms of commonly used bulk quantities, the mean velocity

$$W_m = \frac{1}{S}\int_S W \,\mathrm{d}S \tag{24}$$

and the bulk temperature

$$T_b = \frac{1}{W_m S}\int_S TW \,\mathrm{d}S\,. \tag{25}$$

Also using (22), we obtain

$$H + WG = -\frac{1}{S}\oint_C Q \,\mathrm{d}l + W_m \beta T_b \frac{\mathrm{d}P_h}{\mathrm{d}Z} - W_m \frac{\mathrm{d}P_d}{\mathrm{d}Z} + \rho_m g \beta W_m (T_b - T_m)\,. \tag{26}$$

4 Boundary conditions and solution procedure

4.1 Walls at fixed temperature

With wall temperatures prescribed,

$$T = T_a \quad \text{on the wall} \tag{27}$$

where T_a may vary around the perimeter of the duct but not streamwise, we may seek a solution with $G = H = 0$ so that the energy equation becomes

$$k\nabla_h^2 T + \mu(\nabla_h W).(\nabla_h W) = \Pi W, \tag{28}$$

where $\Pi = \beta T_m \rho_m g$ in Schneider's [2] formulation but $\Pi = 0$ according to Barletta [10]. Taking the horizontal Laplacian of the momentum equation (12) and substituting in (28), we obtain

$$-\frac{k\mu}{\rho_m g\beta}\nabla_h^2(\nabla_h^2 W) + \mu(\nabla_h W).(\nabla_h W) = \Pi W\,. \tag{29}$$

In differentiating (12) the dynamic pressure gradient and the reference temperature have disappeared: (29) applies regardless of the values of these parameters, and so the fourth-order ODEs for W that MW obtained for the cases of parallel plane walls and a circular duct are consistent with (29) if the pressure work term is neglected. Where the choice of reference temperature and the value of the dynamic pressure gradient do make a difference is in the boundary conditions. Using (1), MW obtained the condition

$$\frac{\mathrm{d}^2 W}{\mathrm{d}Y^2} = 0 \quad \text{at the wall} \tag{30}$$

from (27); however, if T_m is used as the reference temperature, (12) indicates that a boundary condition on second derivatives of W must involve T_m if the wall temperature is given. But the cross-section mean temperature T_m is not known *a priori*, whereas the dynamic pressure gradient may be specified (by a mechanical pump in an engineering application); equation (10) relates this pressure gradient to the first derivative of W at the wall. However, this can only be used to provide a useful boundary condition if symmetry considerations (uniform wall temperature as well as geometric symmetry) dictate that $\partial W/\partial n$ has a uniform value around the circumference of the duct: the only geometries in which this is applicable would appear to be parallel plane walls and a circular cross-section, i.e. the two cases considered by MW. The solution procedure to be adopted then depends on whether the symmetry requirements are met.

In the symmetrical configurations, (10) becomes

$$\frac{\mathrm{d}W}{\mathrm{d}Y} = \pm\frac{L}{\mu}\frac{\mathrm{d}P_d}{\mathrm{d}Z} \quad \text{on plane walls at } Y = \pm L \tag{31}$$

or

$$\frac{\mathrm{d}W}{\mathrm{d}R} = \frac{L}{2\mu}\frac{\mathrm{d}P_d}{\mathrm{d}Z} \quad \text{on a circular wall at } \; R = L\,. \tag{32}$$

The no-slip condition is also required:

$$W = 0 \quad \text{on plane walls at } \; Y = \pm L \quad \text{or on a circular wall at } \; R = L\,. \tag{33}$$

MW noted that symmetry implied conditions on the mid-plane between plane walls,

$$\frac{\mathrm{d}W}{\mathrm{d}Y} = 0 \quad \text{and} \quad \frac{\mathrm{d}^3W}{\mathrm{d}Y^3} = 0 \quad \text{at } \; Y = 0, \tag{34}$$

and on the axis of a circular cylindrical duct,

$$\frac{\mathrm{d}W}{\mathrm{d}R} = 0 \quad \text{and} \quad \frac{\mathrm{d}}{\mathrm{d}R}\left(\frac{1}{R}\frac{\mathrm{d}}{\mathrm{d}R}\left(R\frac{\mathrm{d}W}{\mathrm{d}R}\right)\right) = 0 \quad \text{at } \; R = 0\,. \tag{35}$$

These conditions are correct, but what MW did not realise is that they are sufficient to specify that the temperature on the walls is uniform. Thus MW invoked a spurious condition on the second derivative of W, while neglecting to impose the wall shear stress conditions (31) or (32) which would set the first derivative of W to zero on the walls in the case of passive convection. In any case, we now have sufficient boundary conditions to solve (29) for $W(Y)$ in $0 < Y < L$ or for $W(R)$ in $0 < R < L$. The temperature variation $(T - T_m)$ over the cross-section can then be obtained from (12); since this will yield the value of $T_a - T_m$, the temperature distribution can finally be recast in terms of the given wall temperature T_a.

In any less symmetrical geometry, or if there is any spatial variation in wall temperature, the wall shear stress $\mu\partial W/\partial n$ will not be uniform. An iterative solution procedure is then required. The mean temperature T_m is first estimated, and this estimate is used in (12), together with the known wall temperature and pressure gradient, to yield a boundary condition involving the second normal derivative of W at the wall ($\nabla_h^2 W$ will not involve derivatives parallel to the wall, since $W = 0$ at the wall, but it may also involve the first as well as the second normal derivative if the wall is curved). Equation (29) is then solved with this boundary condition and the no-slip condition, and the result is used to compute $\partial W/\partial n$ at all points on the wall. The right-hand side of (10) can then be evaluated, and will in general not match the known pressure gradient. So a new estimate of T_m is made, and the procedure is repeated until (10) is satisfied to within a desired tolerance.

4.2 Heat flux boundary conditions

If the heat flux is prescribed at the wall, the energy equation is

$$k\nabla_h^2 T + \mu(\nabla_h W).(\nabla_h W) = H + GW + \Pi W \tag{36}$$

where the constants H and G relating to temporal and longitudinal temperature variations are to be determined, and Π is fixed, possibly zero. As before, we substitute the horizontal Laplacian of the momentum equation (12) into this, to obtain

$$-\frac{k\mu}{\rho_m g\beta}\nabla_h^2(\nabla_h^2 W) + \mu(\nabla_h W).(\nabla_h W) = H + GW + \Pi W\,. \tag{37}$$

The heat flux boundary condition,

$$k\frac{\partial T}{\partial n} = -Q \quad \text{at the walls,} \tag{38}$$

becomes a condition on third derivatives of W,

$$\frac{\partial}{\partial n}(\nabla_h^2 W) = \frac{\rho_m g\beta Q}{k\mu} \quad \text{at the walls,} \tag{39}$$

in which only the normal derivatives in the Laplacian are non-zero at the wall. Note that if the flow is to be fully developed, the prescribed heat flux Q cannot vary streamwise but may vary horizontally around the wall perimeter. If Q is uniform and the duct geometry is symmetrical, the condition (39) becomes

$$\frac{\partial^3 W}{\partial y^3} = \pm\frac{\rho_m g\beta Q}{k\mu} \quad \text{at plane walls, } Y = \pm L \tag{40}$$

or

$$\frac{\mathrm{d}}{\mathrm{d}R}\left(\frac{1}{R}\frac{\mathrm{d}}{\mathrm{d}R}\left(R\frac{\mathrm{d}W}{\mathrm{d}R}\right)\right) = \frac{\rho_m g\beta Q}{k\mu} \quad \text{at a circular cylindrical wall, } R = L\,. \tag{41}$$

We also have the no-slip condition, $W = 0$ on the walls, and the wall shear stress condition (10) arising from the prescribed dynamic pressure gradient. In the symmetrical configurations these take the forms (31) – (33), and the conditions (34) and (35) continue to apply on the mid-plane or axis of the duct.

The energy equation (36) contains two undetermined parameters, H and G. One such parameter can be determined by an iterative process, similar to that used to determine T_m

when the wall temperature is prescribed. The inability to determine both parameters is a consequence of assuming an infinite duct, with no entry and exit conditions on the temperature; such conditions would determine G (proportional to the streamwise temperature gradient), leaving only H (proportional to the local rate of temperature rise) to be diagnosed from the solution of (37) with the given boundary conditions. However, the usual procedure is to assume that $H = 0$ in an infinite duct and then diagnose G [7]. In a future paper we shall present solutions in which G is assumed zero and H is diagnosed; it would also be possible to obtain a solution with some assumed relation between G and H. In any case, if we assume that one of these quantities has been set to zero or otherwise fixed, the iterative procedure then involves estimating the other one, solving (36) with the no-slip and heat flux boundary conditions, and evaluating the right-hand side of (10). The process is repeated with improved estimates of H or G until the right-hand side of (10) equates to the prescribed dynamic pressure gradient to within the desired precision. The same procedure is required even in a symmetrical configuration, although obviously in that case the calculations are simpler, for example $\partial W/\partial n$ is uniform in (10).

If the heat flux is specified on all walls, the definition of "passive convection" would require that heat flux to be set to zero, i.e. insulated walls. Thermodynamic considerations indicate that no non-trivial passive convection flow is possible in this case: the system is thermodynamically closed and dissipative, so any initial motion will decay until the fluid comes to rest. Proving mathematically that there is no non-trivial solution of the momentum and energy equations with insulated walls and zero applied pressure gradient is not so simple, however, except in the case of parallel plane walls. Setting $Q = 0$ in (40) and $\mathrm{d}P_d/\mathrm{d}Z = 0$ in (31), we have

$$\frac{\mathrm{d}W}{\mathrm{d}Y} = 0 \quad \text{and} \quad \frac{\mathrm{d}^3W}{\mathrm{d}Y^3} = 0 \quad \text{at} \;\; Y = \pm L, \tag{42}$$

which are of the same form as the symmetry conditions at the mid-plane (34). Thus the mid-plane is indistinguishable from an insulated, zero-stress wall, and we can apply the symmetry argument again to show that conditions of the same form must apply at $Y = \pm L/2$. Repeating this argument indefinitely, we see that $\mathrm{d}W/\mathrm{d}Y = 0$ where Y equals any

multiple of $L/2^n$ for arbitrarily large n; so $\mathrm{d}W/\mathrm{d}Y = 0$ everywhere, and the no-slip condition then yields $W \equiv 0$.

4.3 Boundary conditions of the third kind

If the heat flux at the walls is determined by Newton's Law of Cooling [13], then

$$-k\frac{\partial T}{\partial n} = h(T - T_a) \quad \text{at the walls} \tag{43}$$

where the ambient temperature T_a and the cooling coefficient h may vary around the perimeter of the duct but not in the streamwise direction (for fully developed flow). Using (12), this becomes

$$k\frac{\partial}{\partial n}(\nabla_h^2 W) + h\nabla_h^2 W = \frac{h}{\mu}\left(\frac{\mathrm{d}P_d}{\mathrm{d}Z} + \rho_m g\beta(T_a - T_m)\right) \quad \text{at the walls.} \tag{44}$$

The temperature does not vary streamwise, so (29) still applies, and the solution procedures for both symmetric and non-symmetric configuations are the same as when wall temperatures are prescribed. In the non-symmetric case, the iterative method involves solving (29) with the no-slip condition and (44), with T_m in the latter estimated so as to yield a solution satisfying the wall shear-stress condition (10) as closely as possible. With symmetric geometry and boundary conditions, the solutions for W are exactly the same as with prescribed wall temperatures, but the value of T_m is finally obtained from (44) rather than by simply substituting $T = T_a$ in (12). The appropriate forms of (44) are

$$\pm k\frac{\mathrm{d}^3 W}{\mathrm{d}Y^3} + h\frac{\mathrm{d}^2 W}{\mathrm{d}Y^2} = \frac{h}{\mu}\left(\frac{\mathrm{d}P_d}{\mathrm{d}Z} + \rho_m g\beta(T_a - T_m)\right) \quad \text{at } \; Y = \pm L \tag{45}$$

for parallel plane walls, or

$$k\frac{\mathrm{d}}{\mathrm{d}R}\left(\frac{1}{R}\frac{\mathrm{d}}{\mathrm{d}R}\left(R\frac{\mathrm{d}W}{\mathrm{d}R}\right)\right) + h\frac{1}{R}\frac{\mathrm{d}}{\mathrm{d}R}\left(R\frac{\mathrm{d}W}{\mathrm{d}R}\right) = \frac{h}{\mu}\left(\frac{\mathrm{d}P_d}{\mathrm{d}Z} + \rho_m g\beta(T_a - T_m)\right) \quad \text{at } \; R = L \tag{46}$$

for a circular cylindrical duct.

4.4 Mixed boundary conditions

It is possible that different kinds of boundary condition are imposed on different sections of duct wall. As long as some part of the wall does not have heat flux prescribed, the method outlined above for asymmetric cases with prescribed temperature or Newton's Law of Cooling at the boundaries should be used. As an example, Barletta, Lazzari and Magyari [14] considered a duct with parallel plane walls, with no-slip and prescribed temperature on one wall, but prescribed shear stress and heat flux on the other wall. In fact, this paper follows the procedures that we have recommended, with the reference temperature being the cross-section mean and a prescribed pressure gradient being introduced into the problem via a boundary condition of the form (10) and the momentum equation (12). Although the boundary conditions were asymmetric, they were of a form which allowed the calculations to be done as easily as symmetric cases, without the need for an iterative method.

5 Dimensionless equations

The reference length L is the half-width for a duct with parallel plane walls, the radius for a circular duct, or the hydraulic radius for a duct of more general cross-section. Setting the reference velocity U requires more thought. For forced or mixed convection, a Poiseuille velocity, arising from the balance between the imposed dynamic pressure gradient and viscous stress, is appropriate [13, 15]:

$$U_p = \frac{L^2}{12\mu}\frac{\mathrm{d}P_d}{\mathrm{d}Z}\,. \tag{47}$$

In many studies of forced convection, e.g. [7, 16], the cross-section mean velocity has been used as a reference, which then requires that the dynamic pressure gradient be diagnosed from the solution of the flow equations. This may be reasonable if there is a requirement to achieve a given flow rate, but if the dynamic pressure gradient is the prescribed driver of the flow, then the mean velocity is a consequence to be calculated.

For free convection induced by imposed temperature contrasts or heat flux at the wall, a velocity scale may be obtained from a balance between buoyancy and viscous forces, for

example [6, 17]

$$U_f = \frac{g\beta\Delta T L^2 \rho_m}{\mu} \tag{48}$$

(where ΔT is a reference temperature difference), although Morton [18] used a reference velocity based on heat conduction,

$$U_c = \frac{k}{c\rho_m L}\,. \tag{49}$$

However, none of the above seem appropriate for the case of passive convection with viscous dissipation. For this case, MW derived a reference velocity from the balance between conduction and dissipation in (29) and (37):

$$U_d = \frac{k}{\rho_m g\beta L^2}\,. \tag{50}$$

A reference temperature difference was also derived from this balance, as expressed in (28) and (36):

$$\Delta T_d = \frac{\mu U_d^2}{k} = \frac{\mu k}{(\rho_m g\beta L^2)^2}\,. \tag{51}$$

Thus we define the dimensionless velocity and dimensionless temperature difference as

$$w = \frac{W}{U_d}\,, \qquad \theta = \frac{T - T_m}{\Delta T_d}\,, \tag{52}$$

while dimensionless coordinates and differential operators are

$$y = \frac{Y}{L}, \quad r = \frac{R}{L}, \qquad \widetilde{\nabla_h} = L\nabla_h\,, \quad \widetilde{\nabla_h^2} = L^2\nabla_h^2\,, \quad \frac{\partial}{\partial\tilde{n}} = L\frac{\partial}{\partial n}\,, \quad \mathrm{d}\tilde{l} = \frac{1}{L}\mathrm{d}l\,. \tag{53}$$

The dimensionless form of (37) is then

$$-\widetilde{\nabla_h^2}(\widetilde{\nabla_h^2}w) + (\widetilde{\nabla_h}w).(\widetilde{\nabla_h}w) = \eta + \gamma w + Nw\,, \tag{54}$$

where the dimensionless temporal and streamwise temperature variations are

$$\eta = \frac{(\rho_m g\beta L^3)^2}{\mu k^2}H = \frac{(\rho_m g\beta L^3)^2}{\mu k^2}c\rho_m\frac{\partial T}{\partial t}\,, \quad \gamma = \frac{\rho_m g\beta L^4}{\mu k}G = \frac{c\rho_m^2 g\beta L^4}{\mu k}\frac{\partial T}{\partial Z}\,, \tag{55}$$

and the dimensionless pressure work parameter, introduced by Schneider [2], is

$$N = \frac{(\rho_m g\beta L^2)^2 T_m}{\mu k}\,. \tag{56}$$

Where there is a dynamic pressure gradient, its dimensionless form is

$$\lambda = \frac{\rho_m g \beta L^4}{\mu k} \frac{\mathrm{d}P_d}{\mathrm{d}Z}\,, \tag{57}$$

and the equation (12) which is used to diagnose the temperature difference becomes

$$-\lambda + \theta + \widetilde{\nabla_h^2} w = 0\,. \tag{58}$$

The condition (10), which is needed to check the dynamic pressure gradient in the iterative procedure, has the dimensionless form

$$\lambda = \frac{1}{s} \oint_C \frac{\partial w}{\partial \tilde{n}} \,\mathrm{d}\tilde{l}\,, \tag{59}$$

where the dimensionless cross-section area is $s = S/L^2$. The heat flux boundary condition (39) becomes

$$\frac{\partial}{\partial \tilde{n}} (\widetilde{\nabla_h^2} w) = q \tag{60}$$

where the dimensionless heat flux is

$$q = \frac{(\rho_m g \beta)^2 L^5}{k^2 \mu} Q\,. \tag{61}$$

The boundary condition of the third kind (44) becomes

$$\frac{1}{\mathrm{Bi}} \frac{\partial}{\partial \tilde{n}} (\widetilde{\nabla_h^2} w) + \widetilde{\nabla_h^2} w = \lambda - \theta_a \tag{62}$$

where

$$\theta_a = \frac{T_a - T_m}{\Delta T_d}\,, \tag{63}$$

and the Biot number

$$\mathrm{Bi} = \frac{hL}{k} \tag{64}$$

may vary around the duct perimeter.

In a duct with parallel plane walls the dimensionless differential equations become

$$-\frac{\mathrm{d}^4 w}{\mathrm{d}y^4} + \left(\frac{\mathrm{d}w}{\mathrm{d}y}\right)^2 = \eta + \gamma w + N w\,, \tag{65}$$

$$-\lambda + \theta + \frac{\mathrm{d}^2 w}{\mathrm{d}y^2} = 0\,. \tag{66}$$

If the two walls have the same thermal boundary conditions, the no-slip, shear stress and heat flux boundary conditions become

$$w = 0, \quad \frac{\mathrm{d}w}{\mathrm{d}y} = \pm\lambda, \quad \frac{\mathrm{d}^3 w}{\mathrm{d}y^3} = \pm q \quad \text{at} \;\; y = \pm 1\,, \tag{67}$$

the boundary condition of the third kind is

$$\pm\frac{1}{\mathrm{Bi}}\,\frac{\mathrm{d}^3 w}{\mathrm{d}y^3} + \frac{\mathrm{d}^2 w}{\mathrm{d}y^2} = \lambda - \theta_a \quad \text{at} \;\; y = \pm 1\,, \tag{68}$$

and the mid-plane symmetry conditions are

$$\frac{\mathrm{d}w}{\mathrm{d}y} = 0, \quad \frac{\mathrm{d}^3 w}{\mathrm{d}y^3} = 0 \quad \text{at} \;\; y = 0. \tag{69}$$

In a circular cylindrical duct with no variation of conditions around the circumference, the respective equations and boundary conditions are

$$-\frac{1}{r}\frac{\mathrm{d}}{\mathrm{d}r}\left(r\frac{\mathrm{d}}{\mathrm{d}r}\left(\frac{1}{r}\frac{\mathrm{d}}{\mathrm{d}r}\left(r\frac{\mathrm{d}w}{\mathrm{d}r}\right)\right)\right) + \left(\frac{\mathrm{d}w}{\mathrm{d}r}\right)^2 = \eta + \gamma w + Nw\,, \tag{70}$$

$$-\lambda + \theta + \frac{1}{r}\frac{\mathrm{d}}{\mathrm{d}r}\left(r\frac{\mathrm{d}w}{\mathrm{d}r}\right) = 0\,, \tag{71}$$

$$w = 0, \quad \frac{\mathrm{d}w}{\mathrm{d}r} = \frac{\lambda}{2}, \quad \frac{\mathrm{d}}{\mathrm{d}r}\left(\frac{1}{r}\frac{\mathrm{d}}{\mathrm{d}r}\left(r\frac{\mathrm{d}w}{\mathrm{d}r}\right)\right) = q \quad \text{at} \;\; r = 1, \tag{72}$$

$$\frac{1}{\mathrm{Bi}}\frac{\mathrm{d}}{\mathrm{d}r}\left(\frac{1}{r}\frac{\mathrm{d}}{\mathrm{d}r}\left(r\frac{\mathrm{d}w}{\mathrm{d}r}\right)\right) + \frac{1}{r}\frac{\mathrm{d}}{\mathrm{d}r}\left(r\frac{\mathrm{d}w}{\mathrm{d}r}\right) = \lambda - \theta_a \quad \text{at} \;\; r = 1\,, \tag{73}$$

$$\frac{\mathrm{d}w}{\mathrm{d}r} = 0, \quad \frac{\mathrm{d}}{\mathrm{d}r}\left(\frac{1}{r}\frac{\mathrm{d}}{\mathrm{d}r}\left(r\frac{\mathrm{d}w}{\mathrm{d}r}\right)\right) = 0 \quad \text{at} \;\; r = 0. \tag{74}$$

6 Symmetric two-dimensional solutions

We restrict our detailed calculations to the case of flow between parallel plane walls at equal temperatures (although the solutions can be interpreted as applying where Newton's Law of Cooling applies at the walls: see section 4.3). Thus there may be mechanical forcing, but there is no thermal forcing. We are particularly interested in the case of passive convection, where there is a self-sustaining flow without any mechanical or thermal forcing; however, we shall present solutions for the full range of admissible values of the dimensionless dynamic pressure gradient λ. The solutions in Section 6.1 are with the pressure work term neglected, but this term is included in the solutions presented in Section 6.2.

6.1 Solutions neglecting pressure work

With prescribed wall temperatures or Newton's law of Cooling, $\eta = \gamma = 0$ in (65), and we also take $N = 0$ here. Thus (65) reduces to

$$-\frac{\mathrm{d}^4 w}{\mathrm{d}y^4} + \left(\frac{\mathrm{d}w}{\mathrm{d}y}\right)^2 = 0\,. \tag{75}$$

The boundary conditions that we require are the symmetry conditions (69) and the no-slip and shear-stress conditions from (67); as explained above, in the symmetrical case a thermal boundary condition should only be used to determine the relation between the mean temperature and the wall or ambient temperature *after* solving for the velocity profile. We now follow Barletta, Magyari and Keller [12] in writing

$$v = \frac{\mathrm{d}w}{\mathrm{d}y}, \tag{76}$$

so that (75) becomes

$$\frac{\mathrm{d}^3 v}{\mathrm{d}y^3} = v^2\,, \tag{77}$$

to be solved with the boundary conditions

$$v = 0, \quad \frac{\mathrm{d}^2 v}{\mathrm{d}y^2} = 0 \quad \text{at} \;\; y = 0, \tag{78}$$

$$v = \lambda \quad \text{at} \;\; y = 1\,; \tag{79}$$

the dimensionless velocity profile may then be obtained, using the no-slip condition, from

$$w(y) = -\int_y^1 v(y')\,\mathrm{d}y'\,. \tag{80}$$

The temperature profile may be obtained, using (66) and (76), from

$$\theta = \lambda - \frac{\mathrm{d}v}{\mathrm{d}y}\,. \tag{81}$$

Note that the temperature gradient,

$$\frac{\mathrm{d}\theta}{\mathrm{d}y} = -\frac{\mathrm{d}^2 v}{\mathrm{d}y^2}\,, \tag{82}$$

is non-positive and increasing in magnitude with y (from (77) and the second condition in (78)): the temperature decreases monotonically from a maximum at the mid-plane of the duct to a minimum at the wall, and the heat flux by conduction increases towards the wall.

This problem has been solved, both numerically and analytically, by Barletta, Magyari and Keller [12], but with a different choice of reference temperature so they did not pick out the passive convection case within their more general solution. They used a shooting method, whereby the missing initial condition

$$\frac{\mathrm{d}v}{\mathrm{d}y} = \alpha \quad \text{at} \;\; y = 0 \tag{83}$$

is posed and the value of some chosen parameter is then determined as a function of α. In our formulation, which differs from that in [12], that parameter is the dimensionless pressure gradient λ in the boundary condition at $y = 1$. The function of α may, in principle, then be inverted to obtain the value(s) of α required to yield any given value of λ.

The analytical solution of (77) – (79) given in [12] is in the form of a power series, which may be written

$$v(y;\alpha) = \sum_{k=0}^{\infty} C_k \alpha^{k+1} y^{4k+1} \,, \tag{84}$$

in which coefficients C_k are given by a nonlinear recurrence relation:

$$C_0 = 1, \quad C_k = \frac{1}{4k(16k^2-1)} \sum_{j=0}^{k-1} C_j C_{k-j-1} \,. \tag{85}$$

This is essentially the solution that was found subsequently by MW, although they did not cite the earlier work.

It appears not to have been noted previously that the parameter α may be scaled out by means of the change of variables,

$$s = \alpha y^4, \quad U(s) = \frac{v(y;\alpha)}{\alpha y} \,. \tag{86}$$

The solution (84) then becomes

$$U(s) = \sum_{k=0}^{\infty} C_k s^k \,, \tag{87}$$

with coefficients C_k still given by (85), although the differential equation satisfied by $U(s)$ is less concise than (77):

$$64s^2\frac{\mathrm{d}^3U}{\mathrm{d}s^3} + 192s\frac{\mathrm{d}^2U}{\mathrm{d}s^2} + 60\frac{\mathrm{d}U}{\mathrm{d}s} = U^2\,. \tag{88}$$

The initial condition (83) becomes

$$U = 1 \quad \text{at} \;\; s = 0\,, \tag{89}$$

while the other initial conditions (78) are implicit in the change of variables (86); the recurrence relation (85) and the value of C_0 are obtainable by substituting (87) into the differential equation (88) and using (89).

The solution for $U(s)$ is not of much interest in itself, but it holds the key to obtaining all the important parameters. Firstly, we observe that $U(s)$ is a monotonic increasing function. This is clear from the plot of the numerical solution (Figure 1), and can be verified analytically by writing (88) in the form

$$64s^{1/4}\frac{\mathrm{d}}{\mathrm{d}s}\left(s^{1/2}\frac{\mathrm{d}}{\mathrm{d}s}\left(s^{5/4}\frac{\mathrm{d}U}{\mathrm{d}s}\right)\right) = U^2\,, \tag{90}$$

so that

$$\frac{\mathrm{d}U}{\mathrm{d}s} = \frac{1}{64}s^{-5/4}\int_0^s \rho^{-1/2}\int_0^\rho \sigma^{-1/4}(U(\sigma))^2\,\mathrm{d}\sigma\,\mathrm{d}\rho \tag{91}$$

for $s > 0$, while for $s < 0$ we write $\tilde{s} = -s$ and obtain

$$\frac{\mathrm{d}U}{\mathrm{d}\tilde{s}} = -\frac{1}{64}\tilde{s}^{-5/4}\int_0^{\tilde{s}} \rho^{-1/2}\int_0^\rho \sigma^{-1/4}(U(\sigma))^2\,\mathrm{d}\sigma\,\mathrm{d}\rho\,. \tag{92}$$

Since $\sigma^{-1/4}(U(\sigma))^2 \geq 0\;\forall\,\sigma > 0$, it is clear that $\mathrm{d}U/\mathrm{d}s > 0$ and $\mathrm{d}U/\mathrm{d}\tilde{s} < 0$, yielding the monotonicity of $U(s)$ which will be found useful below.

In terms of U, the shear-stress boundary condition (79) becomes

$$U = \frac{\lambda}{\alpha} \quad \text{at} \;\; s = \alpha\,, \tag{93}$$

so that

$$\lambda = \alpha U(\alpha) = \sum_{k=0}^{\infty} C_k\alpha^{k+1}\,. \tag{94}$$

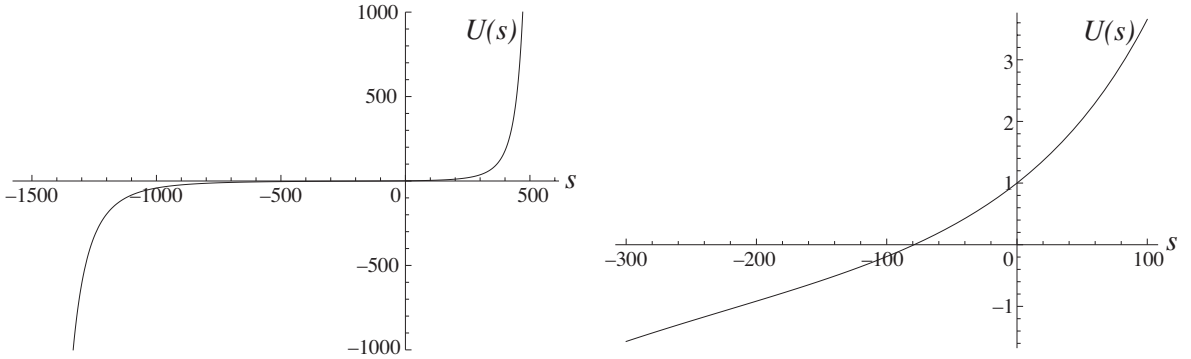

Figure 1: The function $U(s)$, plotted over the domain where $|U(s)| \leq 1000$ and over $-300 \leq s \leq 100$.

Plots of the dimensionless dynamic pressure gradient λ against α are given in Figure 2. [Note that a plot of this function can also be found in [14], Figure 2, where it is the curve for $\Lambda = 0$, but upside-down since our λ is the same as $-\eta$ in [14].] Given a dimensionless pressure gradient λ, these plots yield the corresponding value(s) of α which are required in order to compute the profiles and parameters of physical interest (see below). However, we first note some interesting features of the plots. There is a global minimum of λ, with $\lambda_{\min} \approx -17.1276$ at $\alpha = \alpha_{\mathrm{m}} \approx -36.7908$, while there are two values of α corresponding to any $\lambda > \lambda_{\min}$. These are the dual solutions previously reported by Barletta *et al* [12, 16], although those authors found dual solutions for α given any value of mean upward velocity (below some maximum value) rather than as a function of pressure gradient. While the inability to achieve a volume flux above some maximum level does not give rise to any great conceptual difficulty, it does seem strange in the present formulation that it is impossible to impose a pressure gradient greater than some given level: what happens when one attempts to impose such a pressure gradient, by means of a powerful pump? One might suppose that the symmetry of the flow would break down; however, the same limitation on possible values of pressure gradient was found in [14] for a specifically asymmetric problem, where all the boundary conditions were on the walls, rather than assumed mid-plane symmetry conditions as in the present study. The only remaining possibility is that the assumption

of a steady solution breaks down: the buoyancy force (represented by θ in (66)) is always upwards near the centre-line of the duct, and when this is combined with a large negative pressure gradient (upwards forcing) the viscous stress may be unable to balance these forces. In attempting to provide a balance, large velocity gradients will be set up, generating heat by viscous dissipation at a rate which may be too great to be balanced by conduction out of the duct. Thus there may be a runaway increase in both velocity and temperature, and the momentum and energy equations will need to include terms for the temporal increase in these variables. This will be investigated in a future article.

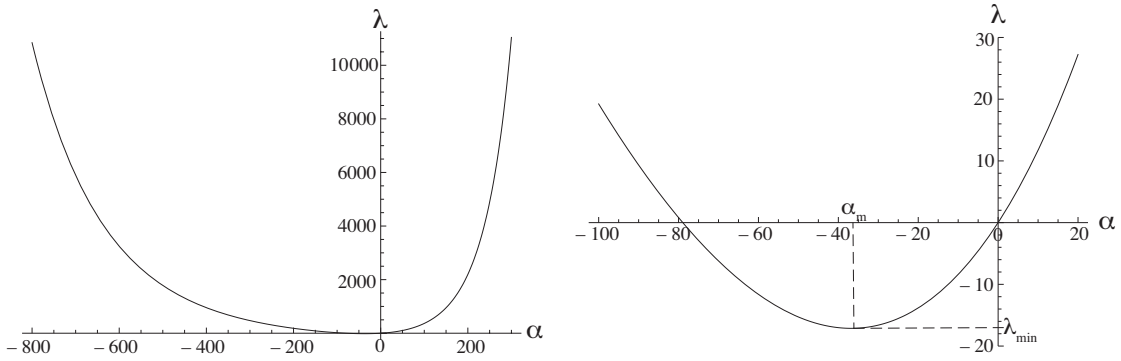

Figure 2: Dimensionless pressure gradient λ as a function of α, plotted on a broad domain and a narrower one.

Another important feature is the zero of λ at $\alpha \approx -78.94547$. Whereas $\lambda = 0$ at $\alpha = 0$ corresponds to the trivial solution $w \equiv 0$, a non-zero value of α with $\lambda = 0$ signifies a non-trivial flow with zero dynamic pressure gradient. This flow has been found previously by Barletta, Lazzari and Magyari [14], who denoted it as "fully separated flow". They described it as being "sustained only by the synergic effects of buoyancy and viscous dissipation": in other words, this is the true passive convection flow. Velocity and temperature profiles in this flow may be found in Figure 4 in [14]. Note that the context is slightly different in [14], where the plane $y = 0$ is supposed to be a wall with boundary conditions identical to those at the plane of symmetry in the present context; Barletta *et al* did recognise that these wall conditions could also be considered as conditions at a plane of symmetry.

Previous authors who have obtained the power series solution (84), (85) have not considered its convergence. A Domb-Sykes plot of the first 500 C_k coefficients (not shown) indicates a radius of convergence of approximately 573.4 (i.e. the series converges for $|s| = |\alpha y^4| \lessapprox 573.4$). The numerical routine used to solve (88) estimates that there is a singularity at $s = 573.433$, and Figure 1 also suggests a singularity in $U(s)$ at some $s > 500$. This figure also suggests the existence of a singularity for negative s, which the numerical routine places at $s = -1534.65$. Since the wall is at $y = 1$, this means that all possible solutions have $-1534.65 \lessapprox \alpha \lessapprox 573.43$, where we recall that

$$\alpha = \left.\frac{\mathrm{d}^2 w}{\mathrm{d}y^2}\right|_{y=0} = \lambda - \theta|_{y=0}\,. \tag{95}$$

We shall denote the locations of the positive and negative singularities of $U(s)$ as s_∞ and $\widetilde{s_\infty}$ respectively, or as α_∞ and $\widetilde{\alpha_\infty}$ when U is being considered as a function of α; i.e.

$$s_\infty \equiv \alpha_\infty \approx 573.433, \qquad \widetilde{s_\infty} \equiv \widetilde{\alpha_\infty} \approx -1534.65\,. \tag{96}$$

The power series solution for $U(s)$ is valid for $|s| < s_\infty$, but is difficult to compute accurately when s approaches $\pm s_\infty$. However, we now derive an asymptotic approximation which is valid near the singularities, i.e. for large positive λ on both branches of the dual solution; this only leaves a range of s values less than $-s_\infty$ but not close to $\widetilde{s_\infty}$ for which no analytical approximation to $U(s)$ is available.

To obtain the asymptotic approximation, it is best to return to the equation (77) for $v(y)$. We suppose that there is a singularity at $y = y_\infty$ with

$$v(y) \sim \kappa(y_\infty - y)^{-n} \tag{97}$$

for some κ and $n > 0$ to be determined. [Note that y_∞ depends on α but is definitely positive, regardless of the sign of α.] Differentiating three times and substituting into (77), we obtain $n = 3, \kappa = 60$. The change of variables $s = \alpha y^4$ yields

$$s - s_\infty \sim 4\alpha(y - y_\infty)^3 \quad \text{as} \;\; y \to y_\infty\,. \tag{98}$$

Substituting $v(y) = \alpha y U(s)$ (from (86)) into (97) then yields

$$U(s) \sim -3840 s_\infty^2 (s - s_\infty)^{-3} \quad \text{as} \;\; s \to s_\infty\,. \tag{99}$$

Expressions (98) and (99) are also valid with s_∞ replaced by $\widetilde{s_\infty}$. From (94) we now have

$$\lambda \sim 3840\epsilon^{-3} \tag{100}$$

where

$$\epsilon = \frac{\alpha_\infty - \alpha}{\alpha_\infty} \quad \text{or} \quad \epsilon = \frac{\widetilde{\alpha_\infty} - \alpha}{\widetilde{\alpha_\infty}} \tag{101}$$

near the positive and negative singularities, respectively, and ϵ is small and positive in both cases. We shall see below that all parameters of physical interest can be expressed as functions of ϵ only, and hence as functions of the dimensionless dynamic pressure gradient λ, as $\alpha \to \alpha_\infty$ or $\alpha \to \widetilde{\alpha_\infty}$; the implication is that when the pressure gradient is very large ($\lambda \to \infty$) the flow is approximately the same on the two solution branches.

Various thermal and flow parameters are now obtained as functions of α, expressed in terms of $U(\alpha)$, as power series solutions valid for $|\alpha| < \alpha_\infty$, and as asymptotic expressions valid as $\lambda \to \infty$; these have all been checked by comparison with numerical solutions. From (80) the velocity profile is

$$\begin{aligned} w(y;\alpha) = -\frac{1}{4}\int_{\alpha y^4}^{\alpha} \left(\frac{\alpha}{s}\right)^{1/2} U(s)\,\mathrm{d}s &= -\sum_{k=0}^{\infty} \frac{C_k}{4k+2}\alpha^{k+1}(1-y^{4k+2}) \\ &= w_0 + \sum_{k=0}^{\infty} \frac{C_k}{4k+2}\alpha^{k+1}y^{4k+2} \end{aligned} \tag{102}$$

where the last form is that obtained by MW, and the velocity on the plane of symmetry is

$$w_0 = -\frac{1}{4}\int_0^{\alpha} \left(\frac{\alpha}{s}\right)^{1/2} U(s)\,\mathrm{d}s = -\sum_{k=0}^{\infty} \frac{C_k}{4k+2}\alpha^{k+1}\,. \tag{103}$$

The cross-section mean velocity (equal to half the volume flux, in dimensionless terms) is

$$w_m = \int_0^1 w(y;\alpha)\,\mathrm{d}y = -\sum_{k=0}^{\infty} \frac{C_k}{4k+3}\alpha^{k+1}\,. \tag{104}$$

If α is close to α_∞ or $\widetilde{\alpha_\infty}$, the dominant contribution to the integral in (102) is from the region where (99) is valid; using this expression for $U(s)$, we obtain

$$w(y;\alpha) \sim -480\epsilon^{-2}\frac{(1-y^4)(1-y^4+\epsilon(1+y^4))}{(1-y^4+\epsilon y^4)^2} \tag{105}$$

in terms of the small parameter defined in (101). This velocity profile has a boundary-layer structure, with

$$w(y;\alpha) \approx -480\epsilon^{-2} \sim -\left(\frac{15}{2}\right)^{1/3}\lambda^{2/3} \tag{106}$$

except in a region of width $\epsilon/4 \sim 60^{1/3}\lambda^{-1/3}$ adjacent to the wall where the velocity adjusts to the no-slip condition. Thus both w_0 and w_m are given by the asymptotic formulae in (106) for large positive values of the dimensionless pressure gradient λ. For moderate values of λ, these flow parameters are plotted against α and against λ in Figure 3. The mechanical forcing is upwards when the pressure gradient λ is negative (which occurs with $-79 \lessapprox \alpha < 0$), whereas on one solution branch the mid-plane and mean velocities are positive (upwards) for a range of positive values of λ (but see the discussion below of the physical accessibility of solutions of this type). Specifically, $w_0 > 0$ when $-284.3105 \lessapprox \alpha < 0$, which corresponds to $\lambda \lessapprox 415.416$ on the upper branch of the solution in Figure 3, while $w_m > 0$ when $-207.4592 \lessapprox \alpha < 0$, corresponding to $\lambda \lessapprox 199.809$ on the upper branch of the solution. The maximum value of w_0 is 28.7715, attained at $\alpha \approx -130.7522, \lambda \approx 57.5431$; the maximum value of w_m is 14.2580, attained at $\alpha \approx -95.1496, \lambda \approx 14.2580$. Note that, from the power-series solutions in (94), (103) and (104),

$$\frac{\mathrm{d}w_0}{\mathrm{d}\alpha} = -\sum_{k=0}^{\infty}\frac{C_k(k+1)}{4k+2}\alpha^k = \frac{1}{4\alpha}(2w_0 - \lambda) \tag{107}$$

and

$$\frac{\mathrm{d}w_m}{\mathrm{d}\alpha} = -\sum_{k=0}^{\infty}\frac{C_k(k+1)}{4k+3}\alpha^k = \frac{1}{4\alpha}(w_m - \lambda)\,; \tag{108}$$

this explains why $w_0 = \frac{1}{2}\lambda$ and $w_m = \lambda$ when the respective flow parameters reach their maximum values.

From (66) the dimensionless temperature profile is given by

$$\theta(y;\alpha) \;=\; \lambda - \frac{\mathrm{d}v}{\mathrm{d}y} = \lambda - \alpha U(\alpha y^4) - 4\alpha^2 y^4 U'(\alpha y^4) \tag{109}$$

$$= \sum_{k=0}^{\infty} C_k \alpha^{k+1}(1 - (4k+1)y^{4k}) \tag{110}$$

where primes denote derivatives. The dimensionless temperatures at the plane of symmetry

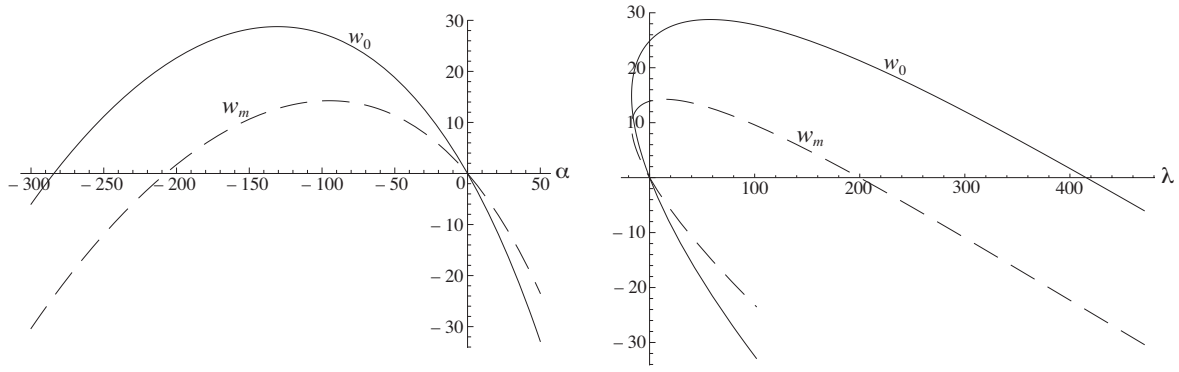

Figure 3: Mid-plane velocity w_0 (solid curves) and cross-section mean velocity w_m (dashed curves), plotted against α and against λ.

$y = 0$ and at the wall $y = 1$ are, respectively,

$$\theta_0 = \lambda - \alpha = \alpha(U(\alpha) - 1) = \sum_{k=1}^{\infty} C_k \alpha^{k+1}\,, \tag{111}$$

$$\theta_1 = -4\alpha^2 U'(\alpha) = -4 \sum_{k=0}^{\infty} k C_k \alpha^{k+1}\,, \tag{112}$$

with asymptotic formulae

$$\theta_0 \sim \lambda\,, \qquad \theta_1 \sim -\left(\frac{9}{20}\right)^{1/3} \lambda^{4/3} \qquad \text{as } \lambda \to \infty\,. \tag{113}$$

The temperature profile has a boundary-layer structure in this asymptotic limit: using the expression (99) for $U(s)$, the second and third terms on the right-hand side of (109) are found to be $O(1)$ except where $\alpha_\infty - \alpha y^4$ is small, which applies only where $y \approx 1$; thus $\theta(y;\alpha) \approx \lambda$ except near the wall. From (66), this implies that in the limit of large downward forcing by the pressure gradient (i.e. $\lambda \to +\infty$), the forcing is balanced by viscous stresses near the wall but by the buoyancy force everywhere else.

The mid-plane and wall temperatures are plotted in Figure 4. These temperatures are relative to the cross-section mean; if we consider the wall temperature to be a fixed boundary condition, temperatures relative to this can easily be obtained by subtraction of (112). Note that $\theta_0 \geq 0$ and $\theta_1 \leq 0$ in all cases; this follows from the monotonicity of the θ profile which

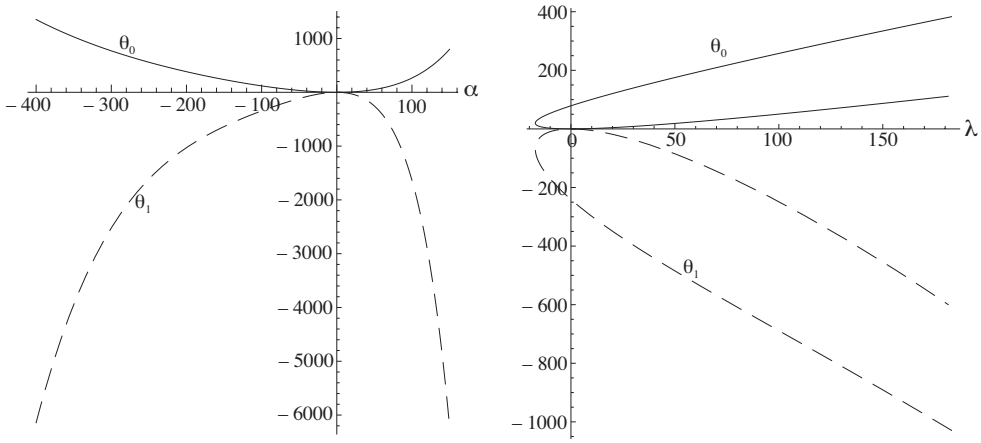

Figure 4: Mid-plane temperature θ_0 (solid curves) and wall temperature θ_1 (dashed curves), both relative to cross-section mean temperature, plotted against α and against λ.

was noted following equation (82), and is also derivable from the expressions in terms of $U(s)$ in (111) and (112), together with the monotonicity of $U(s)$ with $U(0) = 1$.

The heat flux through the wall is, in dimensionless terms, the negative of the temperature gradient there:

$$\left.\frac{\mathrm{d}\theta}{\mathrm{d}y}\right|_{y=1} = -20\alpha^2 U'(\alpha) - 16\alpha^3 U''(\alpha) = -4\sum_{k=0}^{\infty} k(4k+1)C_k\alpha^{k+1}\,, \tag{114}$$

with

$$\left.\frac{\mathrm{d}\theta}{\mathrm{d}y}\right|_{y=1} \sim -\left(\frac{12}{25}\right)^{1/3}\lambda^{5/3} \quad \text{as} \quad \lambda \to \infty\,. \tag{115}$$

This is plotted in Figure 5. Note the "crossover" between the solution branches seen in the plot against λ; a similar crossover also occurs for the wall temperature θ_1, but at a higher value of λ than shown in Figure 4.

The dimensionless bulk temperature is defined here with respect to the half-width of the duct:

$$\theta_b = \frac{1}{w_m}\int_0^1 w\theta\,\mathrm{d}y\,; \tag{116}$$

using (66) and (75), we may obtain

$$\theta_b = \lambda - \frac{1}{w_m}\cdot\left.\frac{\mathrm{d}\theta}{\mathrm{d}y}\right|_{y=1}\,, \tag{117}$$

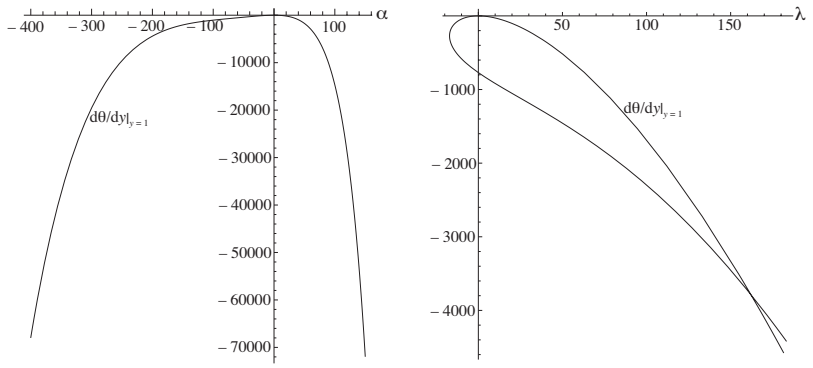

Figure 5: Dimensionless wall heat flux $\mathrm{d}\theta/\mathrm{d}y|_{y=1}$, plotted against α and against λ.

which is a dimensionless version of the integral energy equation (26), omitting the pressure work term and the terms for temporal and streamwise temperature rise. Equation (117) should be used to calculate θ_b once the other parameters have been found from the preceding equations, although an asymptotic formula is available for the case of large pressure gradient:

$$\theta_b \sim \frac{3}{5}\lambda \quad \text{as} \quad \lambda \to \infty \,. \tag{118}$$

We have already observed that the cross-section mean flow speed w_m has two zeroes: at $\alpha = 0$ there is no flow and θ_b is simply zero, but where $w_m = 0$ with bi-directional flow in the duct at a non-zero value of α, the bulk temperature as defined by (116) has a singularity, as seen in the plots of θ_b in Figure 6. Furthermore, θ_b is negative when $-354.9454 \lessapprox \alpha \lessapprox -207.4592$, which corresponds to $199.809 \lessapprox \lambda \lessapprox 704.100$ on the lower solution branch in Figure 6. Since bulk temperature is the convective heat flux normalised by the volume flux, a negative value of θ_b indicates that the net transport of heat is in the opposite direction to the net flow of fluid that is carrying this heat: to resolve this paradox will require examination of velocity and temperature profiles.

Profiles of dimensionless velocity and temperature are shown in Figure 7 for several significant values of α and λ:

- $\alpha = -13.1551, \lambda = -10.4145$: the case erroneously considered by MW to represent passive convection, in which $\mathrm{d}^2w/\mathrm{d}y^2 = 0$ at the wall, $y = 1$;

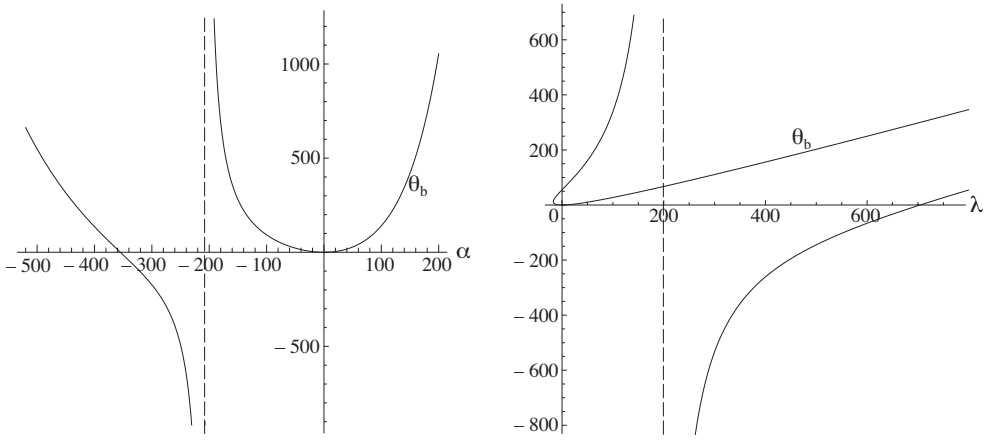

Figure 6: Dimensionless bulk temperature θ_b, plotted against α and against λ. Vertical dashed lines indicate values of α and λ where θ_b is singular.

- $\alpha = \alpha_{\mathrm{m}} = -36.7908, \lambda = \lambda_{\mathrm{min}} - 17.1276$: the greatest negative value of dynamic pressure gradient λ (as found in [14]);
- $\alpha = -78.9455, \lambda = 0$: the true passive convection case (also included in [14]);
- $\alpha = -95.1496, \lambda = 14.2580$, yielding maximum volume flux;
- $\alpha = -130.7522, \lambda = 57.5431$, yielding maximum mid-plane velocity;
- $\alpha = -207.4592, \lambda = 199.809$, yielding zero volume flux;
- $\alpha = -284.3105, \lambda = 415.416$, yielding zero mid-plane velocity (and within the range where bulk temperature is negative);
- $\alpha = -354.9454, \lambda = 704.100$, yielding zero bulk temperature.

We also plot profiles for several positive values of α for which the corresponding values of λ relate to those above:

- $\alpha = 13.7805, \lambda = 17.1276$: dynamic pressure gradient of equal magnitude and opposite sign to its greatest negative value;
- $\alpha = 34.5477, \lambda = 57.5431$: same value of λ that yields maximum mid-plane velocity;

- $\alpha = 73.7580, \lambda = 199.809$: same value of λ that yields zero volume flux;
- $\alpha = 133.3653, \lambda = 704.100$: same value of λ that yields zero bulk temperature.

Finally, to illustrate behaviour in the limit of very large dynamic pressure gradient, we plot profiles for the dual solutions with $\lambda = 10{,}000$, which have $\alpha = -786.9881$ and $\alpha = 294.0599$.

The arrangement of the plots in Figure 7 is as follows. The upper plots contain profiles for values of λ less than or equal to that which yields the maximum mid-plane velocity ($\lambda = 57.5431$); so there is a monotonic decrease of w_0 with α in the velocity profiles in this plot. The middle plots contain profiles with higher values of λ, except for the profiles with $\lambda = 10{,}000$ which are in the lower plots; note the different ordinate scales between the upper, middle and lower plots. Velocity profiles are labelled with the value of α (to the nearest integer). Temperature profiles are not labelled, but the mid-plane temperature θ_0 increases monotonically with $|\alpha|$, with profiles for positive values of α shown dashed; the set of α values used in each temperature plot is the same as those used in the velocity plot to its left.

The behaviour on the solution branch with $\alpha > \alpha_{\mathrm{m}}$, which we shall denote as the "$\alpha+$ branch", is straightforward. The velocity is everywhere in the direction of decreasing pressure, and $|w|$ increases monotonically from the wall to the mid-plane; so buoyancy forces due to heat generation by viscous dissipation modify the classical Poiseuille flow profile, but do not completely alter its character. Temperatures similarly increase monotonically from the wall to the mid-plane, with the boundary-layer structure at large values of λ being more apparent in the temperature than the velocity profiles. Viscous dissipation depends on the velocity gradient, which is greatest near the wall: the heat generated here must be removed by conduction through the wall, which requires the steep temperature gradients seen near the wall. The lesser heat generation nearer the mid-plane leads to the flatter temperature profile here.

In contrast, buoyancy forces play a much more dominant role on the "$\alpha-$ branch" (the solution branch with $\alpha < \alpha_{\mathrm{m}}$). For $-284 \lessapprox \alpha \lessapprox -79$, the pressure gradient is forcing the flow downwards but there is a region around the mid-plane of the duct where the flow

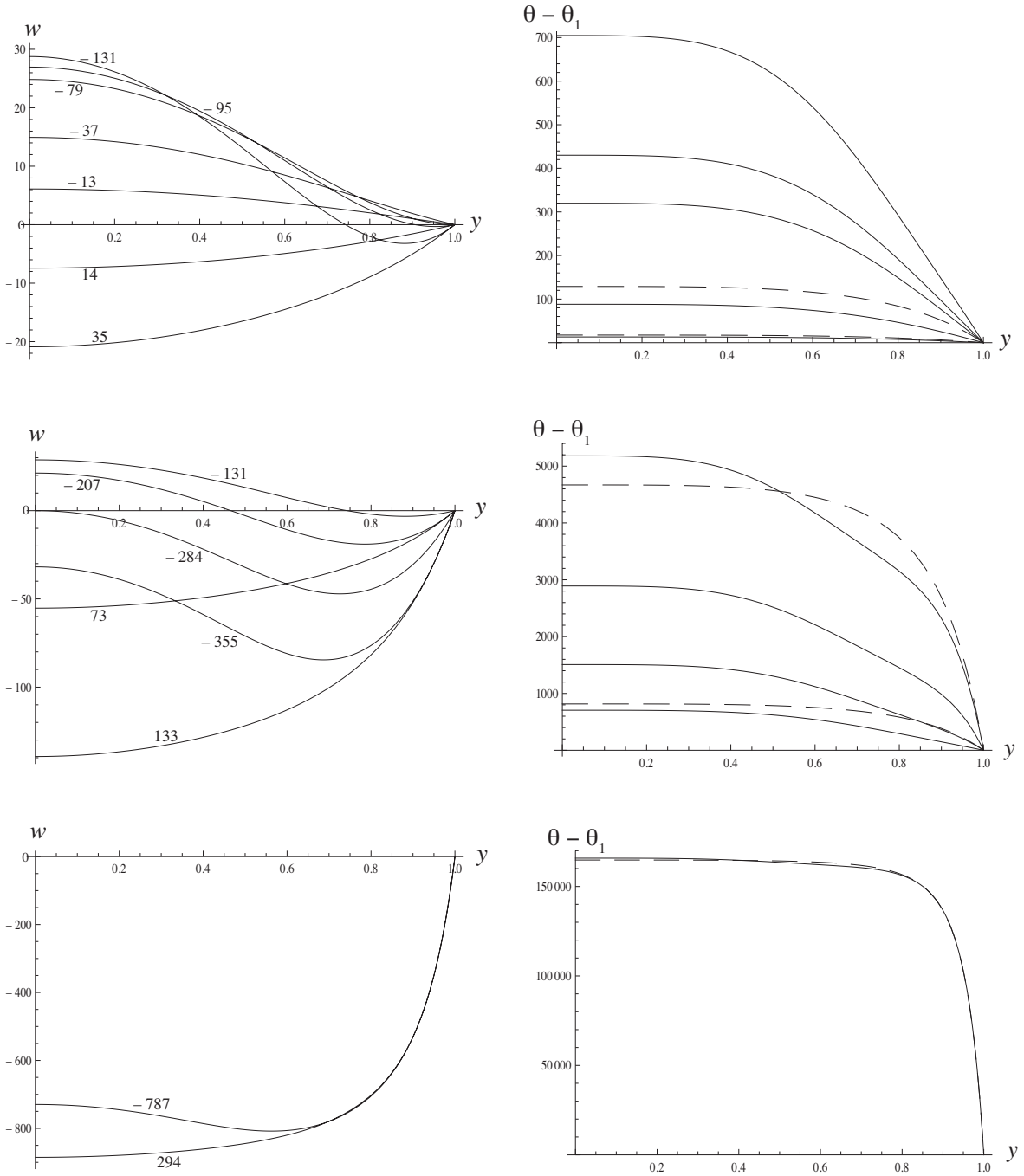

Figure 7: Profiles of dimensionless vertical velocity w (left panels) and dimensionless temperature relative to wall temperature, $\theta - \theta_1$ (right panels). Numerical labels on curves indicates values of α to nearest integer. See text for further explanation.

is upwards. Proof that it is buoyancy forces that are responsible for this comes from the temperature profiles: temperatures are much higher on the $\alpha-$ branch than with the same values of pressure gradient on the $\alpha+$ branch (the dashed profiles in the top right panel of Figure 7 are for flows with the same pressure gradients as the top two solid profiles). Thus not only is passive convection theoretically possible (at $\alpha \approx -79$), but even convection acting against an applied pressure gradient, without any externally applied thermal forcing. Flows on the $\alpha-$ branch have a velocity minimum (if $\alpha \lessapprox -79$) fairly near the wall; between this minimum and the mid-plane there is a region of velocity gradients much steeper than those on the $\alpha+$ branch. It is this steep velocity gradient that is responsible for generating the heat that allows upwards convection flow.

Velocity gradients near the wall are controlled by the pressure gradient through the shear stress boundary condition in (67), and so are the same on both solution branches, being rather large in magnitude and so yielding high rates of heat generation. However, the velocity minimum on the $\alpha-$ branch is also a zero of heat generation, and this accounts for the "three-part" temperature profiles seen in the middle right panel of Figure 7. From the conduction-dissipation balance, equation (28) with $\Pi = 0$, we see that to achieve equilibrium by *removing* heat produced by dissipation in some region requires a curved temperature profile (whereas a uniform temperature gradient would simply conduct heat through the region). So the temperature profiles show a central region of appproximately uniform gradient around the velocity minimum, whereas they are more curved in the regions of steeper velocity gradient on either side of this minimum.

To explain the negative bulk temperatures when $-355 \lessapprox \alpha \lessapprox -207$, we need to compare the velocity and temperature profiles in the middle panels in figure 7. Near the mid-plane there is a region of upward, or relatively small downward, velocities in a mean downward flow, but the mid-plane neighbourhood is also where the highest temperatures are found; so the upward heat transport near the mid-plane is contrary to the overall downward flow.

If the pressure gradient is very large, it must be dominant, and so the differences between the two solution branches become relatively small in this case (Figure 7, bottom panels). A

large pressure gradient requires a large velocity gradient near the wall; the consequent large heat generation requires the large temperature gradient to conduct heat out through the wall. Away from the wall, both velocity and temperature gradients are flatter.

Flows on the $\alpha-$ branch would be difficult to realise. The duct would need to be primed with an upward flow near the mid-plane before applying the pressure gradient. If a pressure gradient was applied to a flow starting from rest, any equilibrium (achievable if $\lambda \gtrapprox -17$) would be on the $\alpha+$ branch because the state of rest is on this branch.

6.2 Solutions including expansion work

We now consider flow between parallel plane walls, again with symmetric prescribed temperatures (or Newton's Law of Cooling) at the walls, but with the pressure work parameter $N > 0$ (noting that $N < 0$ would be unphysical). We still have $\eta = \gamma = 0$ in equation (65), which then becomes

$$-\frac{\mathrm{d}^4 w}{\mathrm{d}y^4} + \left(\frac{\mathrm{d}w}{\mathrm{d}y}\right)^2 = Nw\,, \tag{119}$$

with boundary conditions

$$\frac{\mathrm{d}w}{\mathrm{d}y} = 0, \quad \frac{\mathrm{d}^3 w}{\mathrm{d}y^3} = 0 \quad \text{at} \;\; y = 0\,, \tag{120}$$

$$w = 0, \quad \frac{\mathrm{d}w}{\mathrm{d}y} = \lambda \quad \text{at} \;\; y = 1\,. \tag{121}$$

We cannot reduce the order of the differential equation (119) as was done for the case $N = 0$ (see equations (76) – (80)). Thus the process of recasting as an initial-value problem in order to obtain a power series solution involves the introduction of two initial values,

$$w = w_0 \quad \text{and} \quad \frac{\mathrm{d}^2 w}{\mathrm{d}y^2} = \alpha \quad \text{at} \;\; y = 0\,. \tag{122}$$

The power series solution then involves three parameters (N, α, w_0) rather than the single parameter α in (84); while one of these parameters can be removed by a change of variables similar to (86), this analytical solution does not yield as much insight as in the case $N = 0$, so we shall not present it here.

In equation (119) the pressure work term is linear in w whereas the viscous dissipation term is quadratic; thus, for any non-zero N, the principal energy balance at sufficiently small velocities will be between pressure work and conduction. So if the applied pressure gradient and the consequent velocity magnitudes are small, solutions of (119) with small N may not look like perturbed solutions of (75), the equation that excludes pressure work. If N is of small or moderate magnitude, viscous dissipation will become dominant at greater velocities, with solutions then being similar to those obtained in the absence of pressure work; but if N is sufficiently large, pressure work will be of leading-order importance in all solutions. We shall present some results with $N = 10$ to illustrate the former case, and some with $N = 100$ for the latter. A full analysis of the system of equations (119) – (121), with a complete exploration of (λ, N) parameter space, will be the subject of further research.

One notable difference from the solutions with $N = 0$ is that the temperature is no longer constrained to decrease monotonically from the mid-plane $y = 0$ to the wall $y = 1$. From equation (119) with boundary conditions (120), $\mathrm{d}^3w/\mathrm{d}y^3$ has the opposite sign to w_0 in some region $0 < y < \delta$; since $\mathrm{d}\theta/\mathrm{d}y = -\mathrm{d}^3w/\mathrm{d}y^3$ from (66), the temperature will have a local minimum or maximum at the mid-plane if the flow there is respectively upwards or downwards. Physically, this is because the symmetry condition means that there is no heat generated by viscous dissipation at the mid-plane, while the requirement for pressure work will cool a rising fluid and warm a sinking fluid.

In the absence of pressure work, steady solutions were found not to exist for $\lambda < \lambda_{\min}$, where $\lambda_{\min}$ is a certain negative value of dimensionless pressure gradient: the buoyancy force was upward except near the duct walls, and viscous stresses were unable to maintain a force balance if there was also a large upward pressure forcing. If pressure work is included, the magnitude of $\lambda_{\min}$ increases with increasing N: an upward flow with pressure work entails cooling, decreasing the temperature and hence the upward buoyancy force, and so allowing a larger pressure gradient to be balanced. On the other hand, whereas unbounded positive values of λ were allowed with $N = 0$, steady solutions no longer exist with unbounded downward forcing if $N > 0$: downward velocities now entail heating due to pressure work as

well as by viscous dissipation, so when the downward forcing and the consequent velocities are too great it may become impossible for the removal of heat by conduction to balance the generation of heat by these two mechanisms.

The range of allowed solutions is illustrated for $N = 10$ and for $N = 100$ in Figure 8, where we plot the mid-plane boundary values α and w_0 (see (122)) against λ: compare with Figure 2 (with axes interchanged) and Figure 3. There are now dual solutions for each value of λ between a minimum and a maximum allowed value, and also for each value of α and of w_0 between certain minimum and maximum values. The extreme allowed values with $N = 10$ and with $N = 100$ are listed in Table 1.

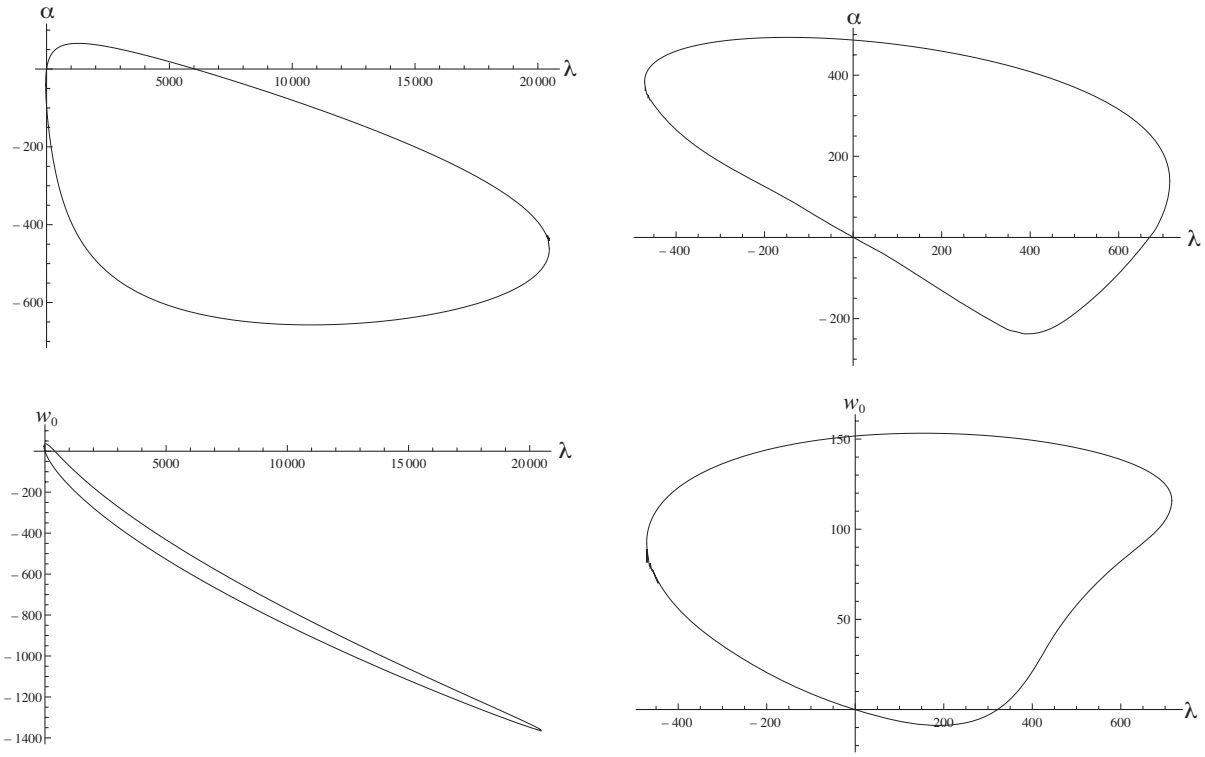

Figure 8: Mid-plane boundary values α (upper panels) and w_0 (lower panels) as functions of dimensionless pressure gradient λ, with $N = 10$ (left panels) and $N = 100$ (right panels).

For $N = 10$, there are many similarities to the results without pressure work, whereas for $N = 100$ the differences are much more marked. Passive convection solutions, with $\lambda = 0$ but $w_0 \neq 0$, exist for both values of N; however, the velocity and temperature profiles (Figure 9)

Table 1: Minimum and maximum values of λ, α and w_0 for which solutions exist with $N = 0$, $N = 10$ and $N = 100$.

	$N = 0$	$N = 10$	$N = 100$
$\lambda_{\min}$	-17.1276	-38.5519	-471.1475
$\lambda_{\max}$	∞	20468.25	715.208
$\alpha_{\min}$	-1534.65	-657.51	-236.538
$\alpha_{\max}$	573.433	65.9442	493.173
$w_{0,\min}$	$-\infty$	-1362.89	-8.4224
$w_{0,\max}$	28.7715	36.1444	153.2386

with $N = 10$ are rather similar to those without pressure work, whereas they are very different when $N = 100$. With $N = 10$, both the mid-plane velocity and temperature are about 50% greater than with $N = 0$, and the profiles are very similar except for the shallow minimum in temperature at the mid-plane with $N = 10$, a necessary consequence of the upward velocity there when pressure work is accounted for. In contrast, the profiles with $N = 100$ show a deep minimum not only in the temperature but also in the velocity at the mid-plane. In this case the heating by viscous dissipation is concentrated in a near-wall region of steep velocity gradients, while cooling due to pressure work produces a downward buoyancy force nearer the mid-plane, resulting in the local minimum of velocity. Temperatures around 20 times as high as for $N = 10$ are required in order to maintain the passive convection against the cooling due to pressure work.

The parameter α is the curvature of the velocity profile at the mid-plane, and Figure 8 shows that this has opposite signs in the cases $N = 10$ and $N = 100$ not only for passive convection, but for any small value of pressure gradient near the origin in the α-λ diagram. For small upward forcing (negative λ), Figure 10 shows that the velocity profile is still Poiseuille-like ($\alpha < 0$) with $N = 10$ as with $N = 0$, but with $N = 100$ there is a mid-plane velocity minimum ($\alpha > 0$). The temperature profiles verify that this is caused by the greater cooling due to pressure work and consequent downward buoyancy force with

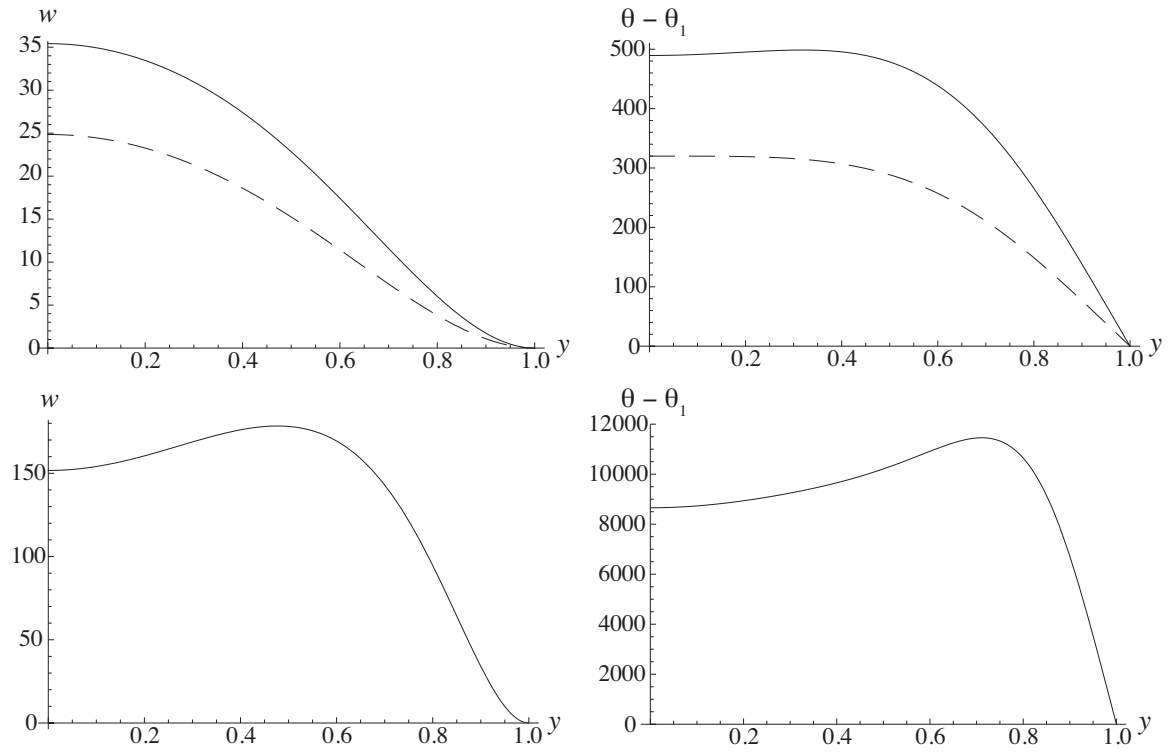

Figure 9: Velocity profiles (left) and temperature profiles (right) for the passive convection solutions with $N = 0$ (dashed lines) and $N = 10$ (solid lines) in the upper panels, and with $N = 100$ in the lower panels, on a different scale.

$N = 100$. Dissipative heating is a much smaller effect when pressure gradients are small, and is only apparent in the temperature profile when $N = 0$.

Other differences between the cases $N = 0$, $N = 10$ and $N = 100$ are apparent when the forcing is greater. The largest value of upward forcing allowed, $|\lambda_{\min}|$, has a roughly two-fold increase over its value in the absence of pressure work when $N = 10$, but is an order of magnitude greater when $N = 100$. With large downward forcing (positive λ), the λ-α plot is qualitatively different when pressure work is included, compared to the case $N = 0$. Without pressure work, two solution branches exist as $\lambda \to \infty$, one with monotonically increasing α and the other with monotonically decreasing (and negative) α; but with $N > 0$, the branches join at $\lambda = \lambda_{\max}$. For $N = 10$, this maximum allowed forcing is very large and yields large downward velocities everywhere, although heating due to pressure work

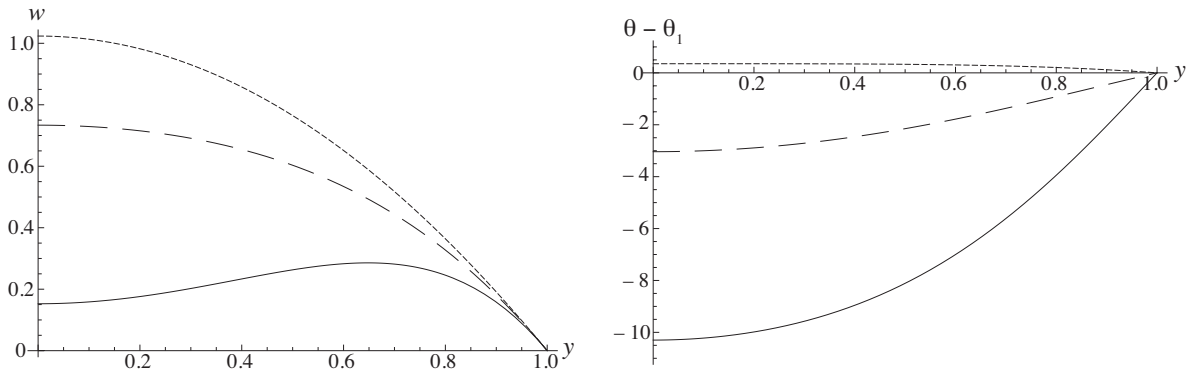

Figure 10: Velocity profiles (left) and temperature profiles (right) with $\lambda = -2$ (small upward forcing), with $N = 0$ (short-dashed lines), $N = 10$ (long-dashed lines) and $N = 100$ (solid lines).

produces an upward buoyancy force which is responsible for negative values of α, i.e. a local minimum in the magnitude of downward velocity at the mid-plane. With $N = 100$ and large downward forcing, the downward flow near the wall leads to such strong pressure work heating, combined with dissipative heating, that the resultant upward buoyancy force produces upward flow near the mid-plane. The maximum sustainable downward forcing is also severely limited when pressure work heating is so strong.

7 Discussion

The claim by Miklavčič and Wang [1] to have found a "passive convection" solution of the equations for flow with viscous dissipation in a vertical duct, and the response by Schneider [2], have highlighted the importance of the choice of reference temperature (or density) when formulating equations and boundary conditions to describe such flows. In previous work, a variety of reference temperatures have been used, including a wall temperature [12, 16], a mean of the temperatures of two walls [15], and the bulk temperature [19]. However, Barletta and Zanchini [3] showed that unless the cross-section mean temperature is used as the reference temperature (as done for example in [7, 14, 20, 21]), unreasonable results may

be obtained for the dynamic pressure gradient, and the velocity profile may also be in error. We have given a rational basis (and a generalisation) for this finding: the reference condition must be hydrostatic equilibrium in order for the dynamic pressure gradient to be correctly diagnosed, and the hydrostatic pressure gradient is determined by the cross-section mean density.

We then presented rational procedures for calculating flows in vertical ducts, assuming that the pressure gradient is prescribed, as is usually assumed in analyses of Poiseuille flow, and as may be the case in engineering applications. With our recommended choice of reference temperature, the dynamic pressure gradient is equated to the wall shear stress and hence provides a boundary condition on the velocity. An alternative procedure, adopted by Barletta *et al* [16, 12], is to suppose the volume flux to be prescribed and later diagnose the pressure gradient (although those authors chose the wall temperature as their reference, so according to [3] the calculated pressure gradient may not be correct). Our procedures might be considered more philosophically satisfying, since the volume flux is the consequence, not the cause, of the pressure gradient. In further work Barletta *et al* [14] did use the procedure we recommend, with the reference temperature taken to be the cross-section mean and with the pressure gradient introduced through a shear stress boundary condition; indeed, they even obtained the true solution for completely passive convection. Miklavčič and Wang were apparently unaware of this solution, maybe because it is contained within an analysis of a much more general problem.

As well as pointing out the problems with MW's choice of reference temperature, Schneider [2] asserted that they should not have neglected the term in the energy equation which accounts for work done when a compressible fluid moves down a pressure gradient. The need to retain this term is a matter of some debate in the literature [9, 10, 11, 22]; the fundamental equations of thermodynamics are not in question, but rather which approximations to the energy equation are consistent with the Boussinesq approximation. We have avoided this question by obtaining solutions both with and without the pressure work term in the energy equation. In particular, we have found passive convection solutions when it is retained as

well as reproducing the solution found by Barletta, Lazzari and Magyari [14] when it is neglected.

Schneider [2] observed that passive convection solutions apparently violate the First Law of Thermodynamics, allowing heat to be extracted (by conduction through the duct walls) when there is no input of heat or work. This is still the case after we have dealt with the issues of reference temperature and pressure work, so Schneider's attribution of the thermodynamic paradox to these issues is not valid. Instead, the resolution of the paradox is this: not only is heat allowed to be extracted, it *must* be extracted. If the heat is not removed, the temperature of the wall (or of the external fluid, if it is a thin wall) will increase in time. With no mechanism to produce a corresponding increase in internal temperatures, this would result in a reduction of temperature gradients within the fluid. Hence there would be a reduction in the buoyancy forces driving the flow and of the consequent viscous dissipation that is generating heat. Thus the system would gradually run down, tending towards a state of no motion and uniform temperature. To maintain "passive" convection within the duct requires active extraction of heat: it is the work done in the external refrigeration unit that constitutes the energy input needed to maintain perpetual motion with heat output. One might argue that this extraction of heat negates the passivity of the convection, but our definition of "passive" only requires that the *imposed* boundary conditions do not provide any forcing. Passive convection is impossible within a thermodynamically closed system (although Turcotte at al [23] did report an "adiabatic flow" in a vertical duct with zero pressure gradient, equal temperatures on the walls and zero heat flux through the walls. Their equations included pressure work as well as viscous dissipation, and their adiabatic solution involved downward flow with the temperature everywhere lower than at the walls – a rather curious result, given that both pressure work and viscous dissipation would tend to warm a descending fluid. They did not comment on the thermodynamic balance of this flow, but since the wall temperature was used as their reference temperature it is possible that the dynamic pressure gradient was not zero as supposed). It is possible that other thermodynamic "paradoxes" reported in the recent literature may also be explained by con-

sidering work done outside the system, although we have not investigated this in detail: the important point is that a system is not thermodynamically closed if the boundary conditions specify the temperature or Newton's Law of Cooling.

It nevertheless remains true that passive convection would almost certainly be impossible to realise in practice, even for a limited time. MW were aware that a duct would somehow need to be primed with the correct flow and temperature profile, since by definition passive convection exists under conditions identical to those under which the fluid could be at rest. It would also be necessary to arrange the entry and exit conditions correctly, for a duct of finite length. Even if these difficulties could be overcome, Schneider noted that the values of physical constants for any real fluid would probably render the condition of passive convection inaccessible. Schneider was concerned with conditions under which the pressure work parameter N is small, to see whether MW's neglect of pressure work could be justified; he found that small values of N are incompatible with reasonable values of the velocity scale U_d, because $N \propto L^4$ while $U_d \propto L^{-2}$, where L is the cross-section length scale of the duct. He concluded that large values of N would be of interest; we have shown that passive convection solutions do exist with large N. Taking values of physical constants for water and glycerine at a temperature $T_m = 20°\mathrm{C} = 293\mathrm{K}$ (the latter fluid chosen because we might expect viscous dissipation to play a more important role in a high-viscosity fluid), we find $N \approx 2.1 \times 10^6 L^4$ for water and $N \approx 2.8 \times 10^4 L^4$ for glycerine, with L in metres; so it is certainly feasible to achieve large values of N with moderately sized equipment ($L \gtrsim 0.1\mathrm{m}$). Indeed, a further reason for needing to consider large values of N is that our scale for temperature variation, given by (51), may be written

$$\Delta T_d = \frac{T_m}{N} \tag{123}$$

and it would certainly not be realistic to have temperature variations greater than absolute temperatures (leaving aside the fact that large temperature variations imply large changes in physical properties, including changes of state!). Yet all our passive convection profiles in Figure 9 have dimensionless temperatures much greater than the value of N, making these profiles clearly infeasible; unless the trend for magnitudes of θ to increase with N reverses

at some higher value of N than we have considered, passive convection would be impossible for this reason.

Other quantities whose magnitudes should be checked for feasibility are velocities and pressure gradients. The velocity scale defined in (50) has the magnitude $U_d \approx 0.28L^{-2}$ for water and $U_d \approx 0.086L^{-2}$ for glycerine (L in metres, U_d in m.s^{-1}), so length scales at least of order 1 metre would be required to keep the velocities in the passive convection profiles (Figure 9) to a reasonable level; but this is not as severe a constraint as implied by the temperature profiles. With regard to the forcing, a useful quantity to consider is the ratio of dynamic to hydrostatic pressure gradients, which should be small in order for the Boussinesq approximation to be valid. From (57), we may write

$$\frac{\mathrm{d}P_d}{\mathrm{d}Z} \Big/ \frac{\mathrm{d}P_h}{\mathrm{d}Z} = \frac{\beta T_m}{N}\lambda, \tag{124}$$

and since $\beta T_m \approx 0.062$ for water and $\beta T_m \approx 0.15$ for glycerine, large values of λ are acceptable if N is similarly large.

In conclusion, while our solutions covering all admissible values of dimensionless pressure gradient λ are of considerable mathematical interest, only those solutions within some neighbourhood of the origin on a λ-α diagram are physically feasible. Dual solutions appear to be a universal feature of the equations for vertical flow with viscous dissipation [16], but the solution branch which does not pass through the origin would be very difficult to realise physically. It is also important to examine the magnitude of temperature variations in a mathematical solution in order to determine whether the predicted flow and temperature profile are physically realisable. For example, those presented in Figure 10 do appear realisable, whereas the passive convection solutions in Figure 9 are not. The parameter N, originally introduced when pressure work was included in the equations, turns out to be useful in determining physical feasibility of solutions. In this context, N is required to be rather large; but we have found that solutions including pressure work with large, or even modest, values of N are radically different from those in which pressure work is ignored, especially with the smaller values of λ which allow physically feasible solutions – see Figure 10. This highlights the importance of resolving the question of whether it is valid to formulate

equations including viscous dissipation but without an explicit pressure work term when the Boussinesq approximation is used.

References

[1] M. Miklavčič and C.Y. Wang, Completely passive natural convection, Z. Angew. Math. Mech. **91**, 601–606 (2011).

[2] Schneider, W. (2011). Comments on M. Miklavčič and C.Y. Wang, Completely passive natural convection, ZAMM 91/7, 601–606 (2011), Z. Angew. Math. Mech. **91**, 1002–1004 (2011).

[3] A. Barletta and E. Zanchini, On the choice of reference temperature for fully-developed mixed convection in a vertical channel, Int. J. Heat and Mass Transfer, **42**, 3169–3181 (1999).

[4] M. Miklavčič & C.Y. Wang, Reply to comments by W. Schneider concerning the paper by M. Miklavčič and C.Y. Wang, Completely passive natural convection, ZAMM 91/7, 601–606 (2011), Z. Angew. Math. Mech. **91**, 1004 (2011).

[5] B. Gebhart and J.C. Mollendorf, Buoyancy-induced flows in water under conditions in which density extrema may arise, J. Fluid Mech., **89**, 673–707 (1978).

[6] S. Ostrach, Laminar natural-convection flow and heat transfer of fluids with and without heat sources in channels with constant wall temperatures, NACA Technical Note 2863 (1952) [retrieved from http://naca.central.cranfield.ac.uk/report.php?NID=4991, January 2013].

[7] A. Barletta, Heat transfer by fully developed flow and viscous heating in a vertical channel with prescribed wall heat fluxes, Int. J. Heat and Mass Transfer, **42**, 3873–3885 (1999).

[8] G.K. Batchelor, An Introduction to Fluid Dynamics (CUP, Cambridge, 1967).

[9] A. Barletta, Comments on a paradox of viscous dissipation and its relation to the Oberbeck-Boussinesq approach, Int. J. Heat and Mass Transfer, **51**, 6312–6316 (2008).

[10] A. Barletta, Local energy balance, specific heats and the Oberbeck-Boussinesq approximation, Int. J. Heat and Mass Transfer, **52**, 5266–5270 (2009).

[11] M. Pons and P. Le Quéré, An example of entropy balance in natural convection, Part 2: the thermodynamic Boussinesq equations, C. R. Mécanique **333**, 133–138 (2005).

[12] A. Barletta, S. Lazzari and E. Magyari, Uni- and bidirectional mixed convection flow regimes described by dual solutions in a vertical duct, Acta Mechanica, **194**, 83–102 (2007).

[13] E. Zanchini, Effects of viscous dissipation on mixed convection in a vertical channel with boundary conditions of the third kind, Int. J. Heat and Mass Transfer, **41**, 3949–3959 (1998).

[14] A. Barletta, S. Lazzari and E. Magyari, Buoyant Poiseuille-Couette flow with viscous dissipation in a vertical channel, Z. Angew. Math. Phys., **59**, 1039–1056 (2008).

[15] A. Barletta, Laminar mixed convection with viscous dissipation in a vertical channel, Int. J. Heat and Mass Transfer, **41**, 3501–3513 (1998).

[16] A. Barletta, E. Magyari and B. Keller, Dual mixed convection flows in a vertical channel, Int. J. Heat and Mass Transfer, **48**, 4835–4845 (2005).

[17] P.C. Sinha, Fully developed laminar free convection flow between vertical parallel plates, Chem. Eng. Sci. **24**, 33–38 (1969).

[18] B.R. Morton, Laminar convection in uniformly heated vertical pipes, J. Fluid Mech. **8**, 227–240 (1960).

[19] A. Barletta, Combined force and free convection with viscous dissipationin a vertical rectangular duct with uniform wall heat flux, Int. J. Heat and Mass Transfer, **42**, 2243–2253 (1999).

[20] A. Barletta, Fully developed mixed convection and flow reversal in a vertical circular duct, Int. J. Heat and Mass Transfer, **45**, 641–654 (2002).

[21] A. Barletta, E. Rossi di Schio and E. Zanchini, Combined forced and free flow in a vertical rectangular duct with prescribed wall heat flux, Int. J. Heat and Fluid Flow **24**, 874–887 (2003).

[22] V.A.F. Costa, thermodynamics of natural convection in enclosures with viscous dissipationn, Int. J. Heat and Mass Transfer, **48**, 2333–2341 (2005).

[23] D.L. Turcotte, D.A. Spence and H.H. Bau, Multiple solutions for natural convective flows in an internally heated, vertical channel with viscous dissipation and pressure work, Int. J. Heat and Mass Transfer, **25**, 699–706 (1982).